Development of Semiconductor Detectors Useful for Synchrotron Radiation

Richard M. Osgood

MIT Lincoln Laboratory

Outline

- Large-format CCDs for X-ray detection
- GM-APD arrays for high-flux applications
- Lateral blooming control in large-format CCDs
- Measurements
- Simulations
- Conclusions

Application of CCDs to X-ray Detection

- Charge-coupled devices (CCDs) are a mature technology
  - Simple, robust pixel allows good spatial resolution, large-format devices
- Back-illuminated Si detectors appropriate for soft x-rays
- Pixelated Si detectors for x-ray spectrometry from space (high spatial resolution)
  - 8000 x-ray colors

X-ray spectroscopy

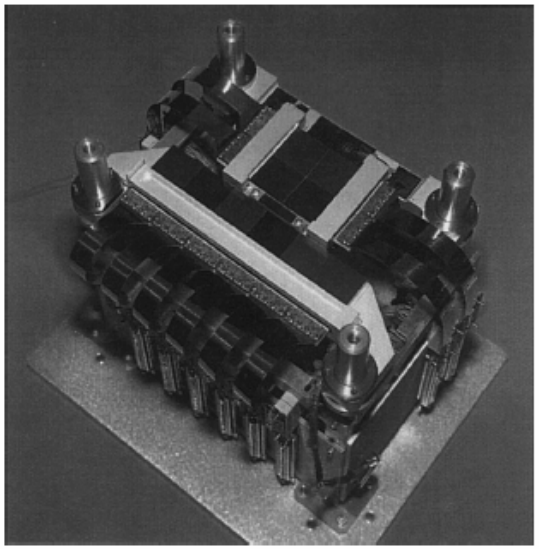

Fig. 1. CCDs used as the AXAF X-ray spectrometer (1×6 array) and X-ray imager (2×2 array). The frame stores are shielded beneath the metal plates.

Charge-coupled devices (CCDs)

- Silicon analog detector
  - Photogenerated charge collected during integration time
  - SiO_2/silicon nitride gate dielectric
  - Incident photons λ > 340 nm generate single electron-hole pairs
- Pixel size 15 μm x 15 μm
- Well under polysilicon phases can contain up to ~ 150 ke^-
- Collecting gates held at V_H collect photoelectrons
- Blocking gates held at V_L to isolate pixels

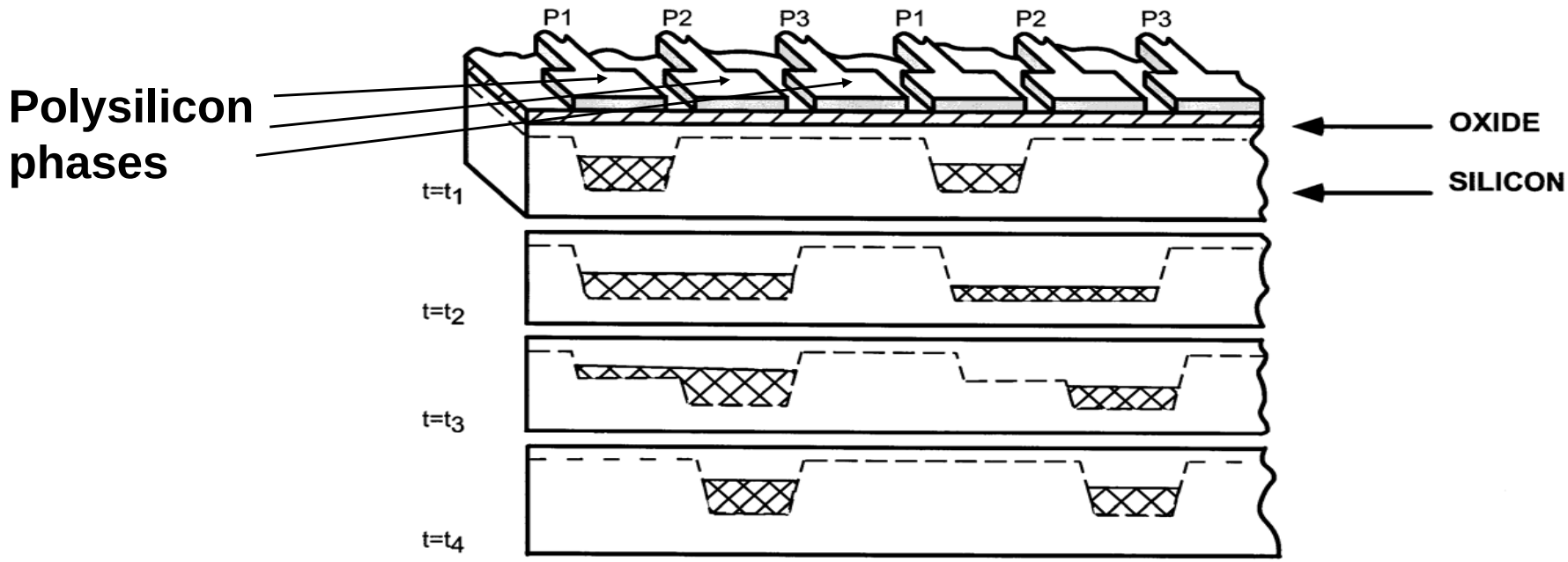

Back-illuminated MITLL CCDs

- **Quantum efficiency of Si back-illuminated (BI) CCDs superior to front-illuminated (FI) CCDs**

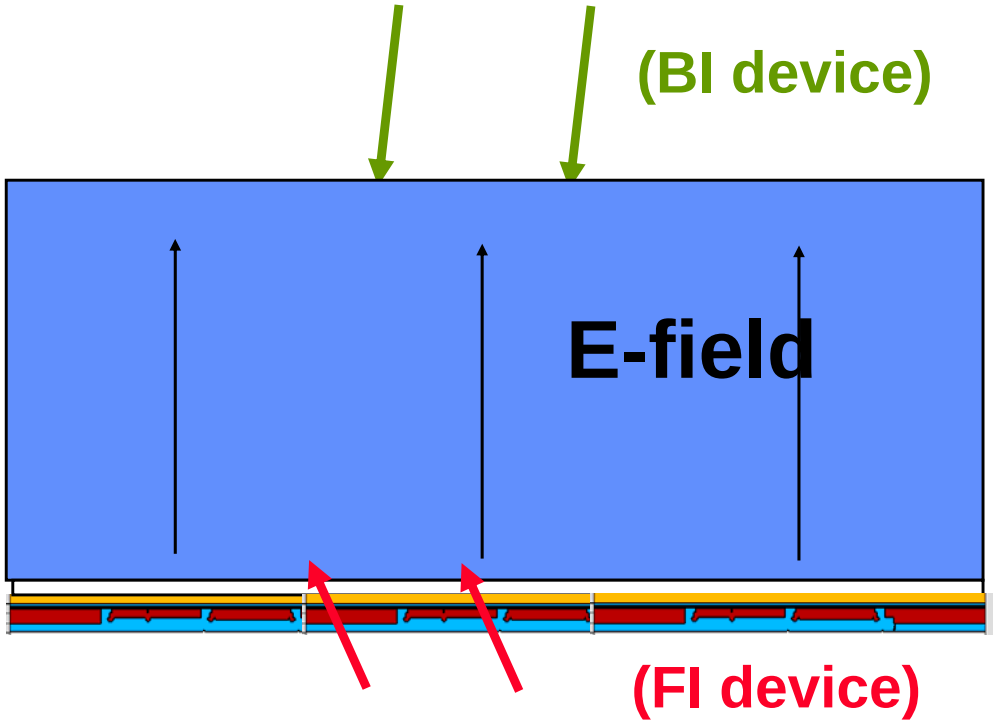

Quantum efficiency of 1998 BI MITLL CCD

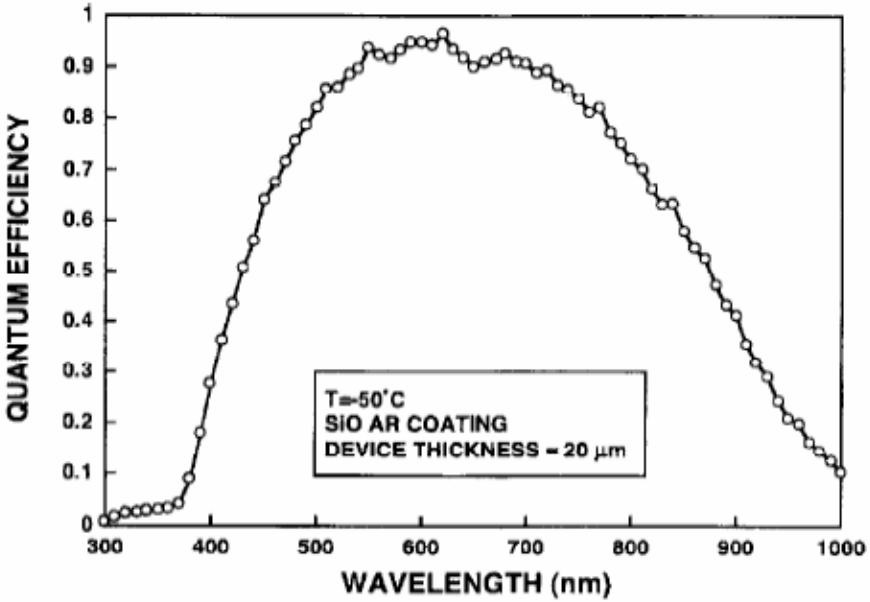

Outline

- Large-format MITLL CCDs for X-ray detection
- GM-APD arrays for high-flux applications
- Lateral blooming control in large-format CCDs
- Measurements and simulations
- Conclusions

Application of GM-APDs to high-flux applications

- **Fast readout**
- **Large dynamic range if frames can be repeated to achieve good statistics for photon interarrival times > about 100 nsec.**

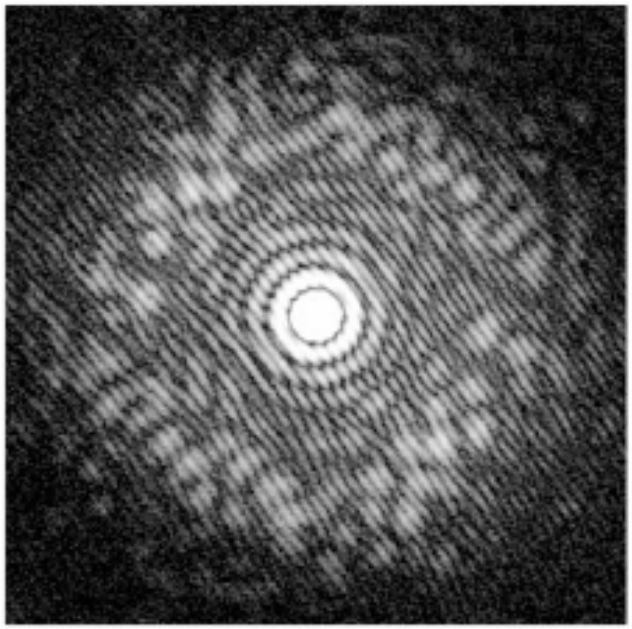

Figure 2 Hologram recorded with X-rays (right circular polarization) at a wavelength of 1.59 nm. The maximum in-plane momentum transfer in the measurement is $\pm 0.13\,\mathrm{nm}^{-1}$, shown up to $\pm 0.06\,\mathrm{nm}^{-1}$ in the image. Intensity is represented on a logarithmic grey scale, with black denoting the minimum intensity of 10^3 and white denoting the maximum intensity of 10^5. Black and white appear saturated in the picture only, the dynamic range of the hologram is 10^7.

Special detector needed for magnetic holography

- Pixelated detector
  - Spatial resolution
- Large-area detector
  - High-frequency components
- Large dynamic range (10^7)
- Saturates at high flux levels (10^8 photons/sec)

Geiger-mode avalanche photodiode (GM-APD)

- p-n photodiode (Si for soft x-rays) biased above breakdown
- Single photon will produce avalanche current
  - Discriminate above noise floor
  - Essentially zero-noise detector
- Caveats
  - Dark count rate
  - Saturation if photon interarrival rate ~ reset time or “dead time”
- Solid-state version of photomultiplier tube
  - Quantum efficiency (Geiger counts/incident photon) can be engineered to be much higher
  - Pixelated: spatial resolution!

P-N Photodiode Avalanche Photodiode

Geiger-mode APDs (GM-APDs)

- **Back-illuminated silicon digital detector**
  - **Photogenerated charge collected during integration time**
  - **SiO_2/silicon nitride gate dielectric**
  - **Incident photons λ > 340 nm generate single electron-hole pairs**
- **Pixel pitch 50 μm or more**
  - **Working on pitches < 50 μm**
- **Fast readout**
- **Probability of detection**

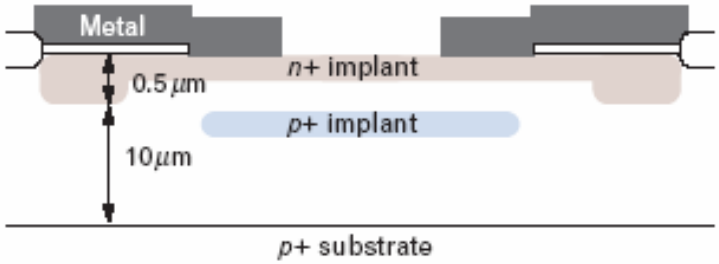

FIGURE 7. Cross-section of the basic APD device structure. The APD is fabricated in a lightly *p*-doped epitaxial layer grown on a heavily *p*-doped (*p*+) substrate. The heavily *n*-doped (*n*+) implant forms the *n*-side contact of the diode and the substrate form the *p*-side contact. The *p*+ implant creates a sheet of charge that segments the structure into regions of low electric field (below the implant), where photon absorption takes place, and high electric field (above the implant), where impact ionization occurs.

Geiger-mode APD array

- GM-APD arrays just entering market place
- Applications: LADAR range imaging (3d), fluorescence sensing and binning, etc.

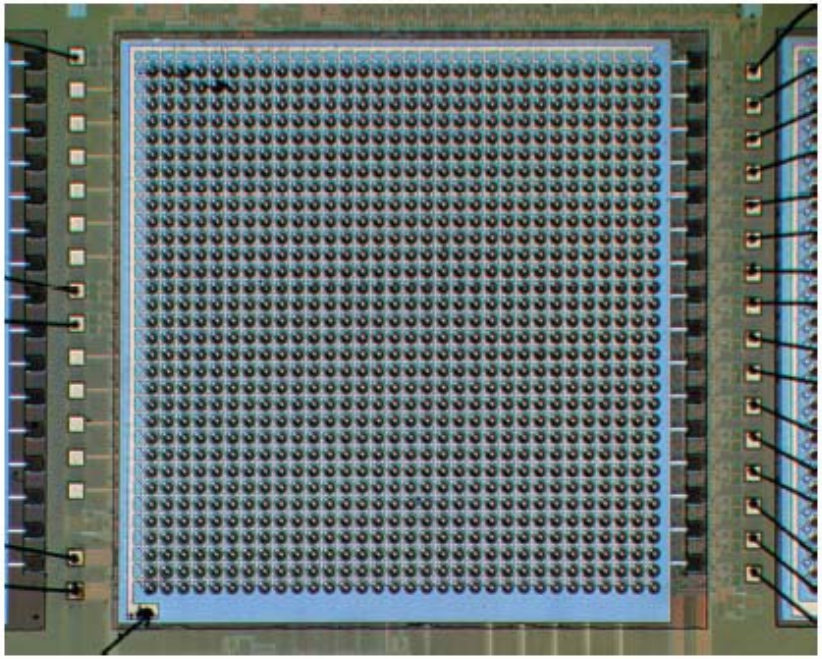

MITLL 32 x 32 GM-APD array

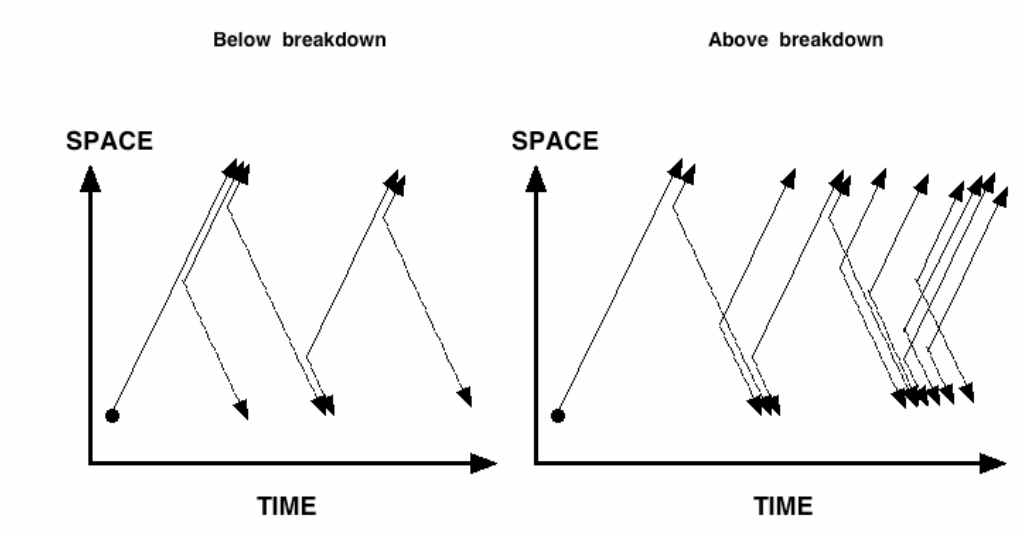

GM-APD reset time

- Want reset time < 10 nsec for photon flux of 10^8 photons/sec
- After firing, GM-APD needs some time to recover before firing again
  - Otherwise probability of firing is artificially enhanced by carriers in trapped states ("afterpulsing").
- Quench circuit keeps GM-APD below breakdown for a certain reset time (a.k.a. "dead time") .
  - Related to how long charge trapped in oxide states needs to de-trap.
  - Longer at lower temperatures.

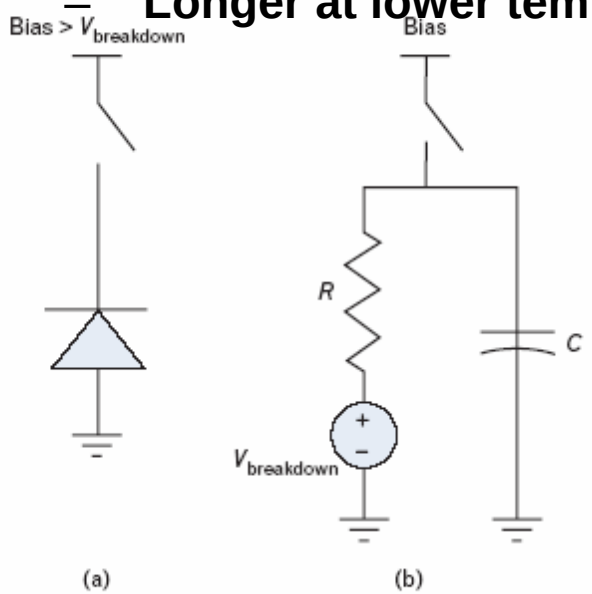

FIGURE 5. Passive-quenching circuits. (a) In Geiger mode, the APD is charged up to some bias above the breakdown voltage V and then left open circuited. (b) Subsequently, once an avalanche has been initiated, the APD behaves according to a simple circuit model.

GM-APD

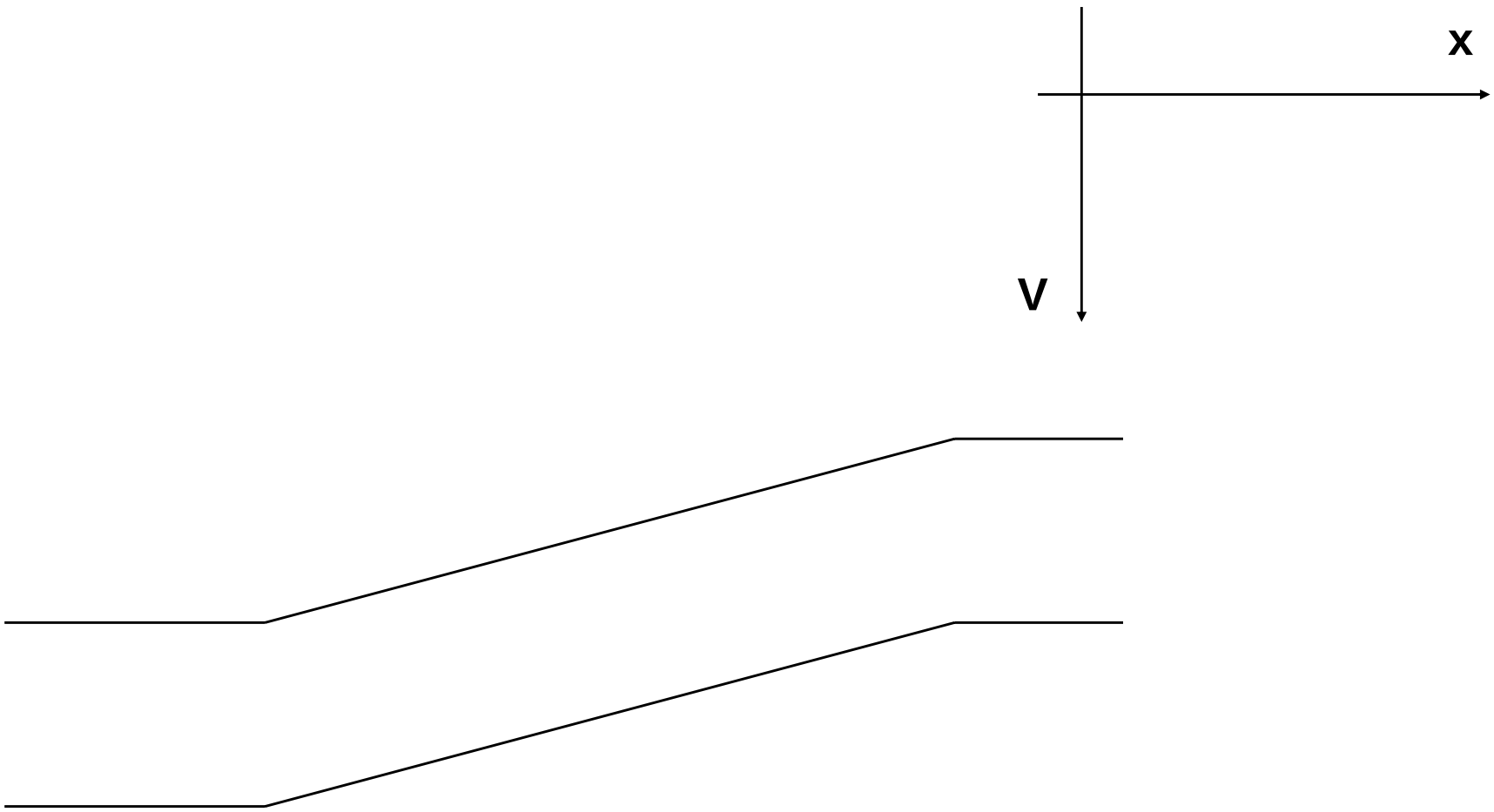

GM-APD

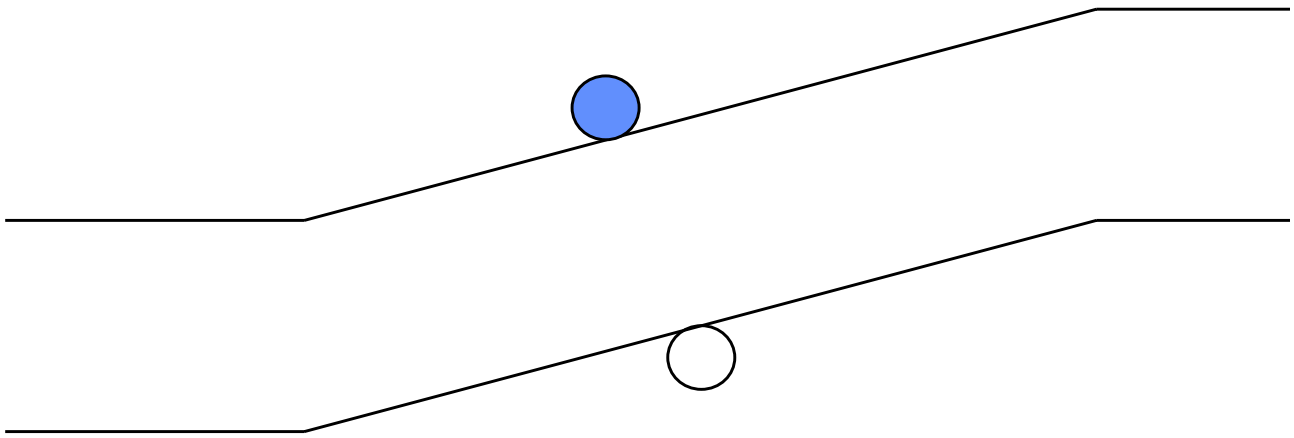

GM-APD

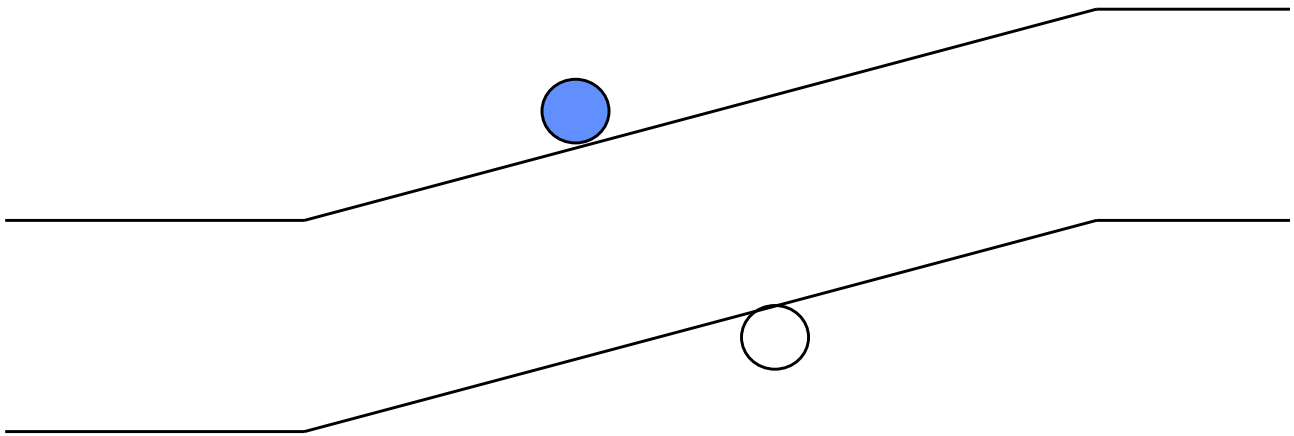

GM-APD

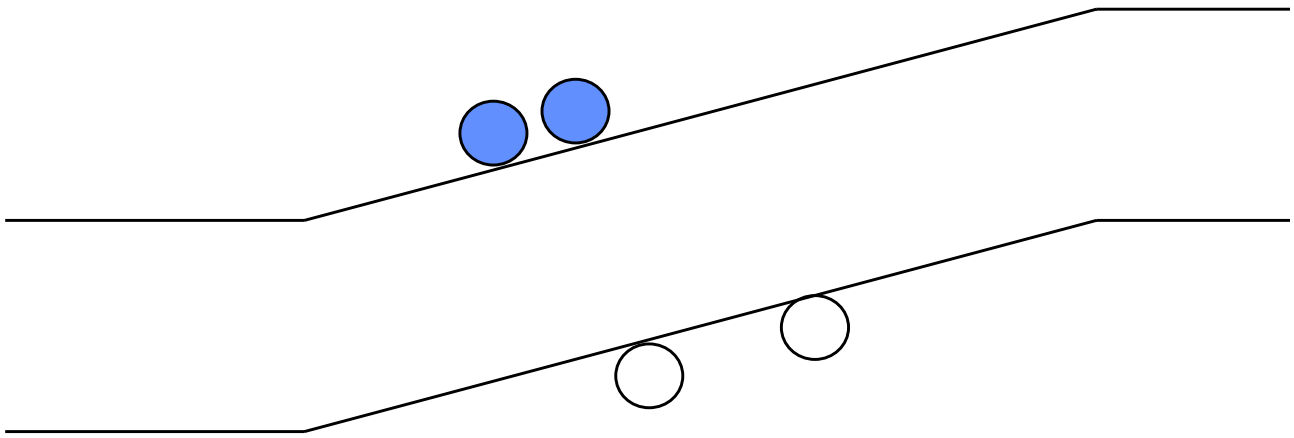

GM-APD

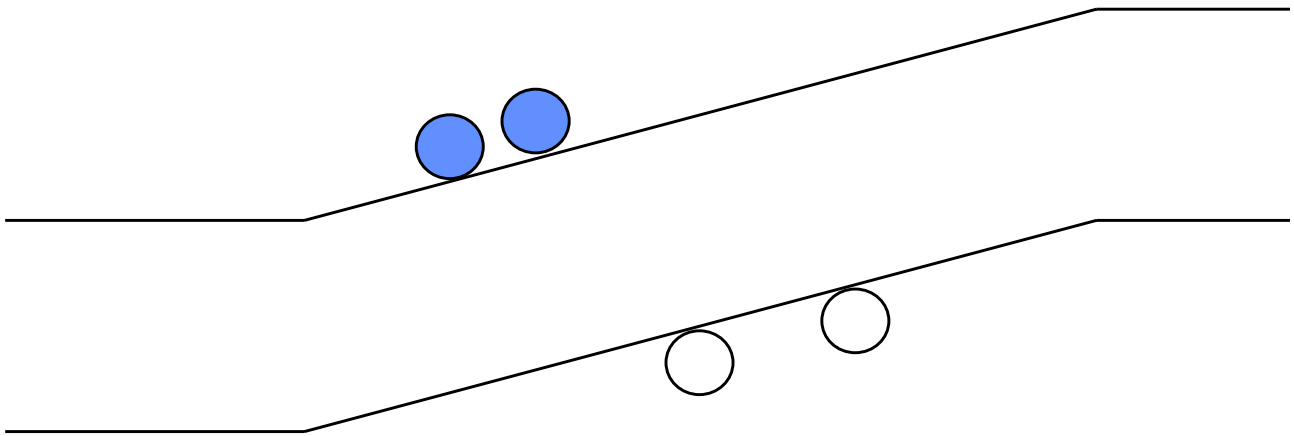

GM-APD

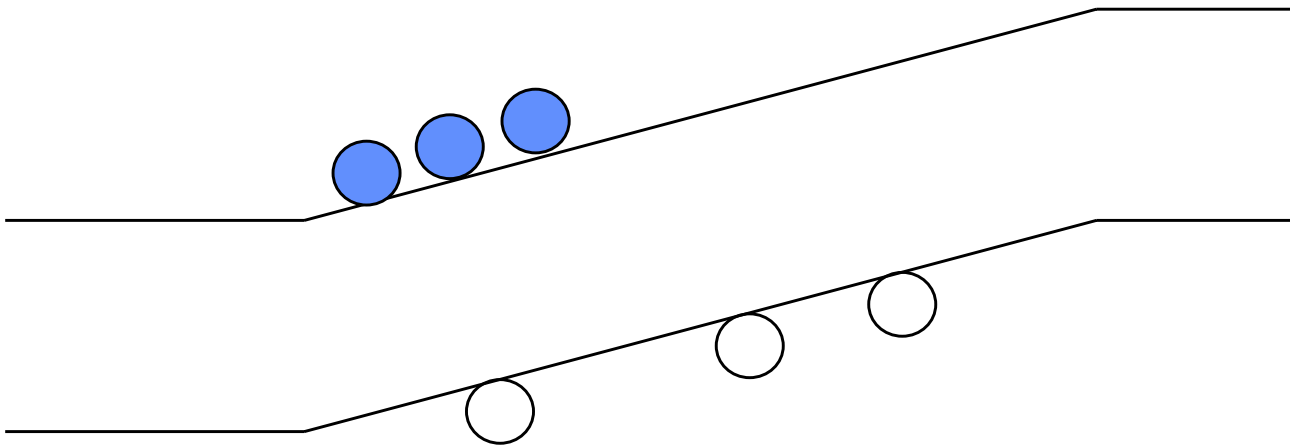

GM-APD

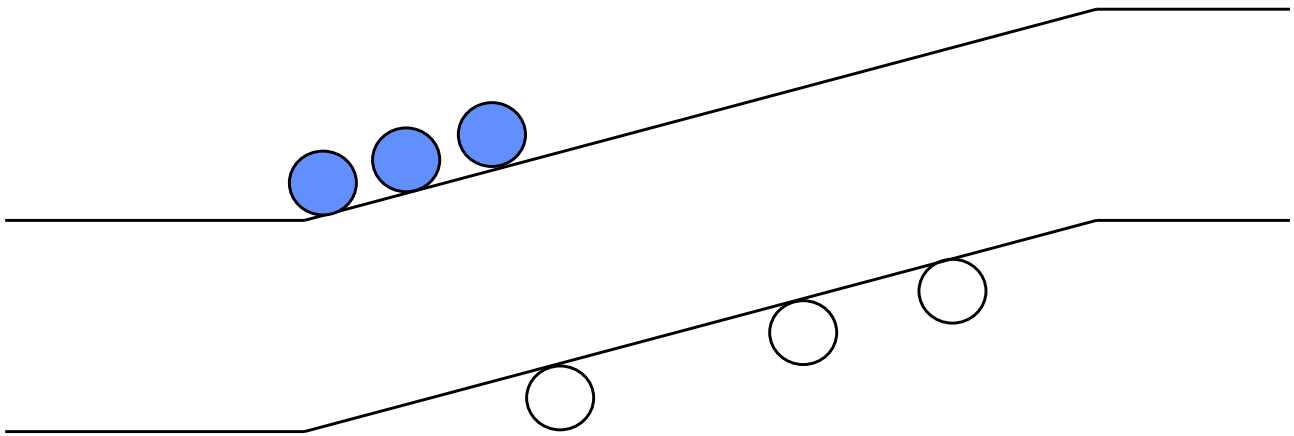

GM-APD

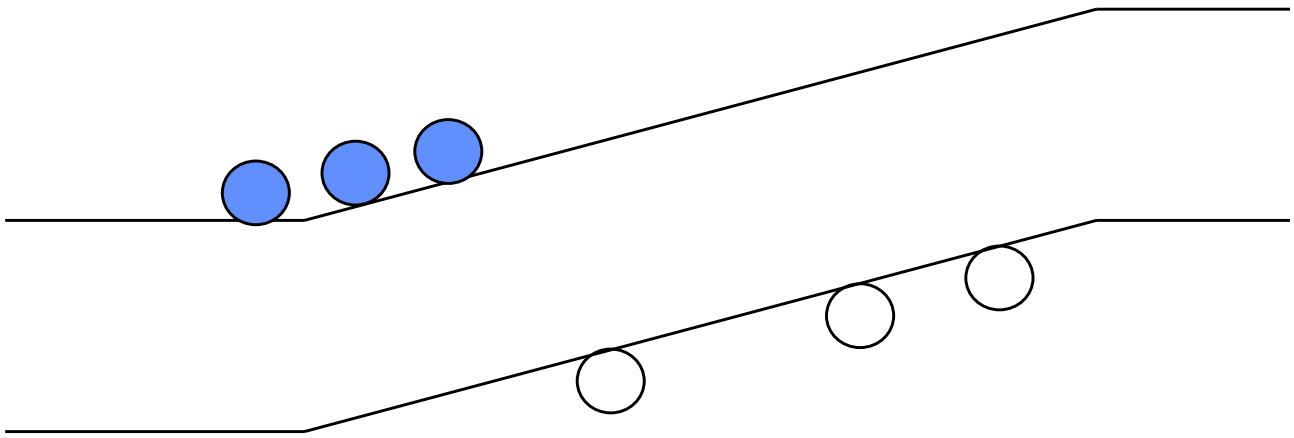

GM-APD

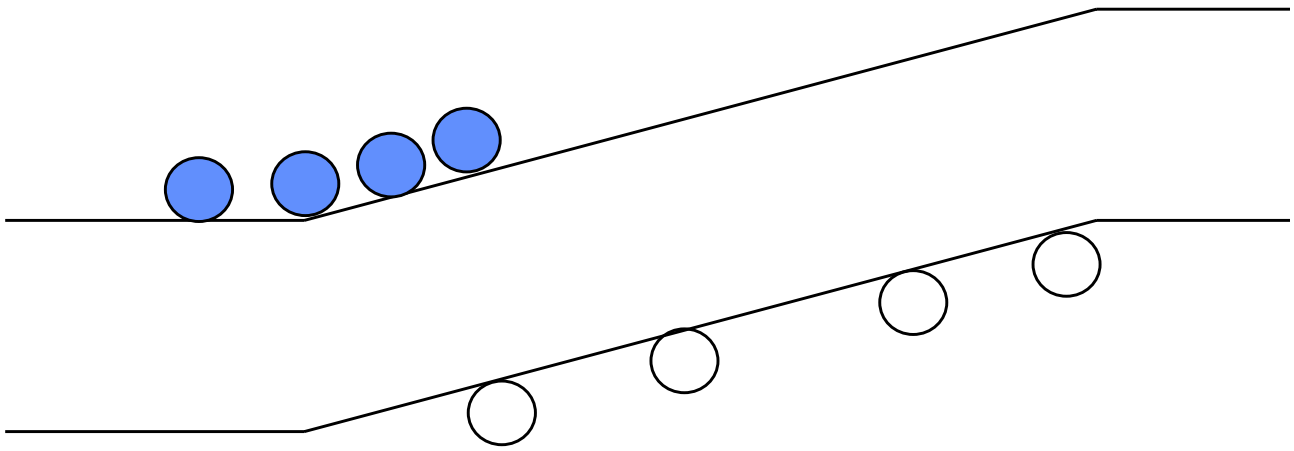

GM-APD

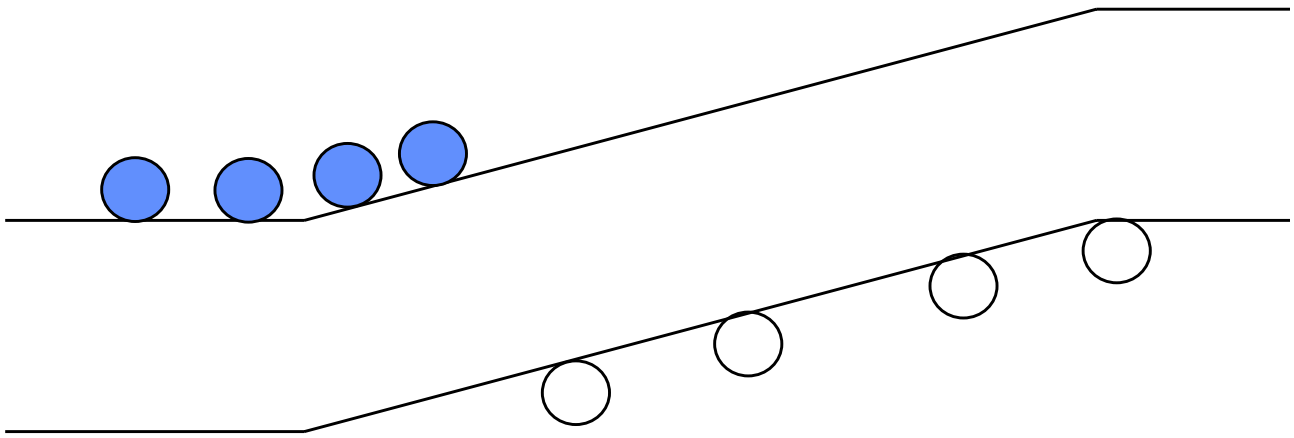

GM-APD

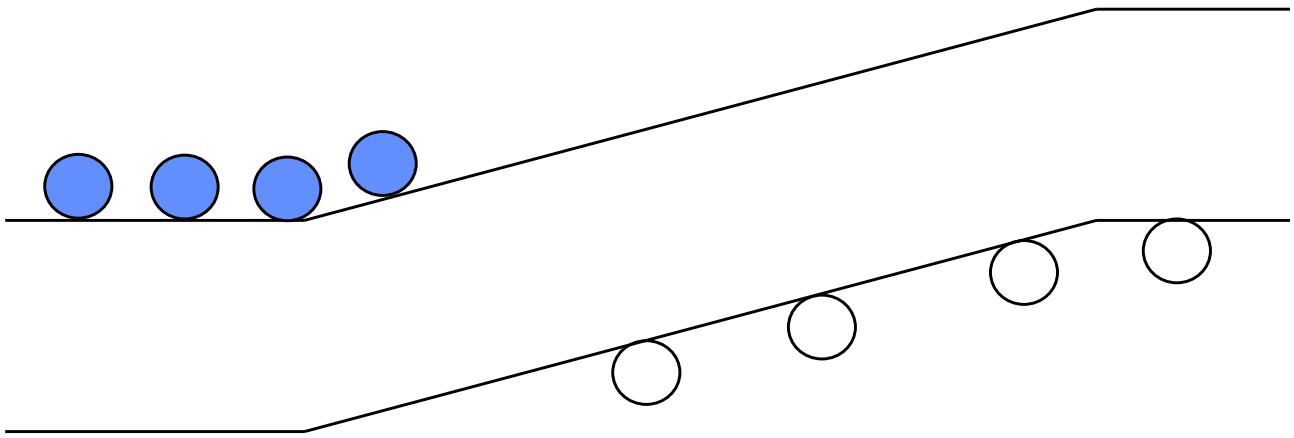

GM-APD

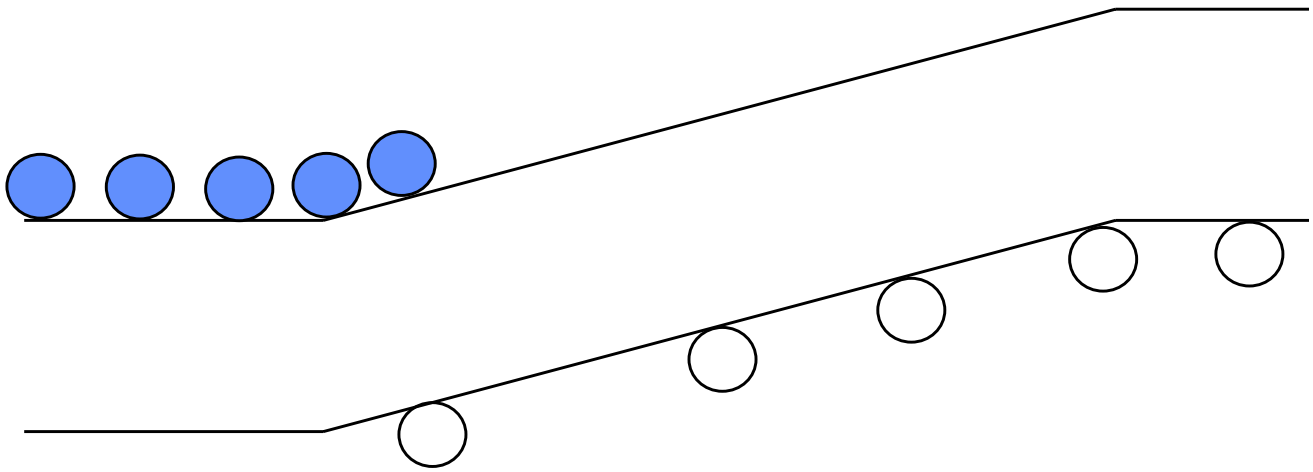

GM-APD

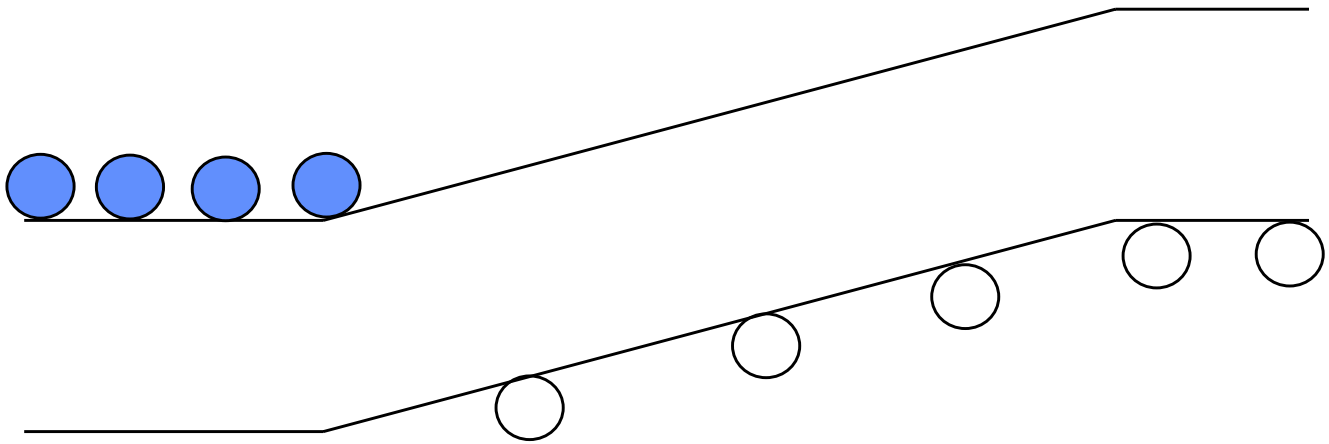

GM-APD

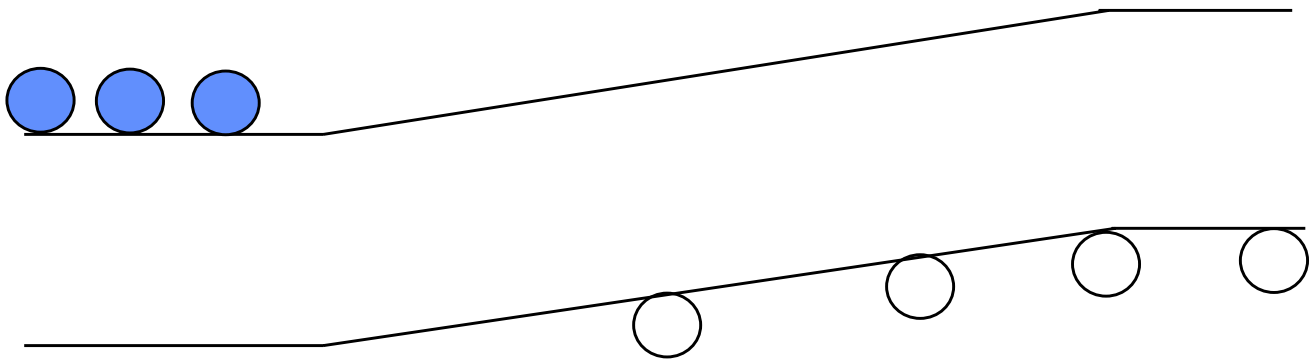

GM-APD

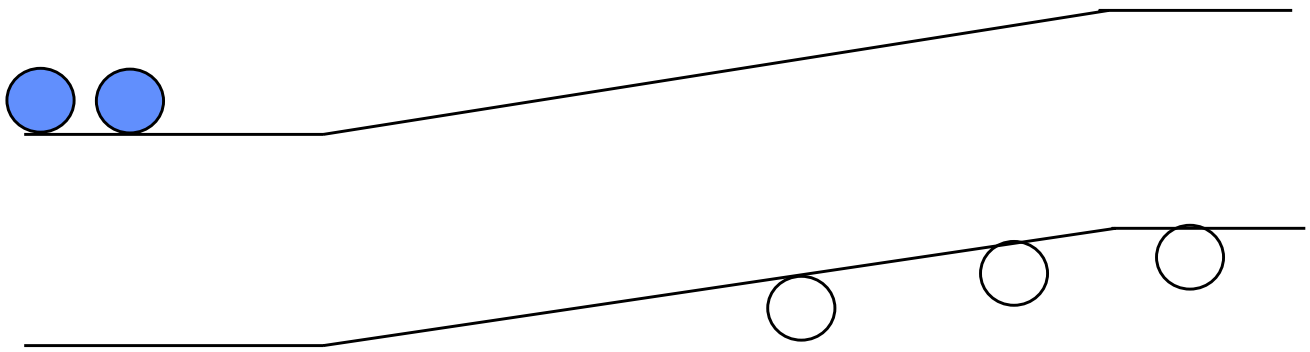

GM-APD

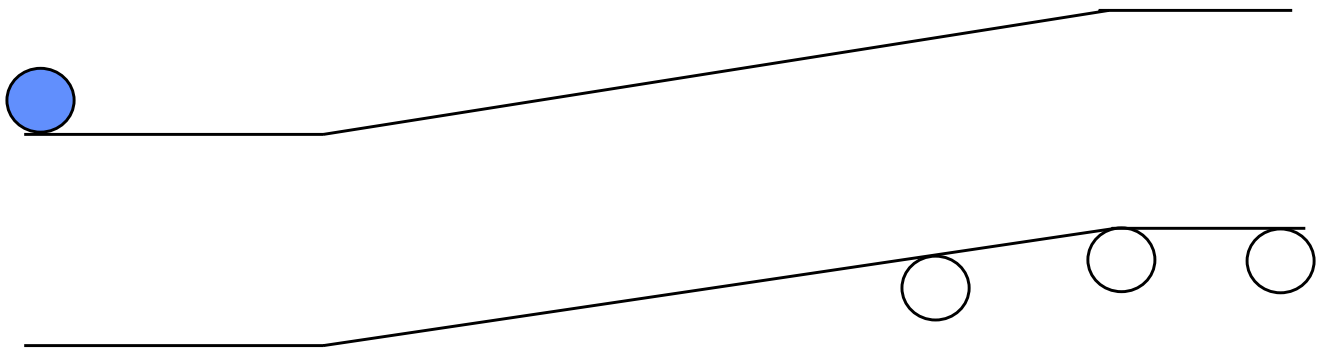

GM-APD

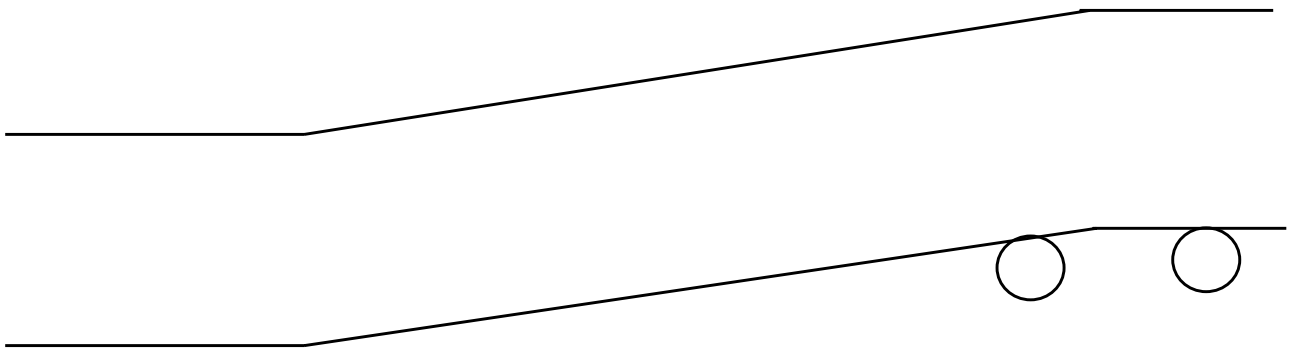

GM-APD reset time

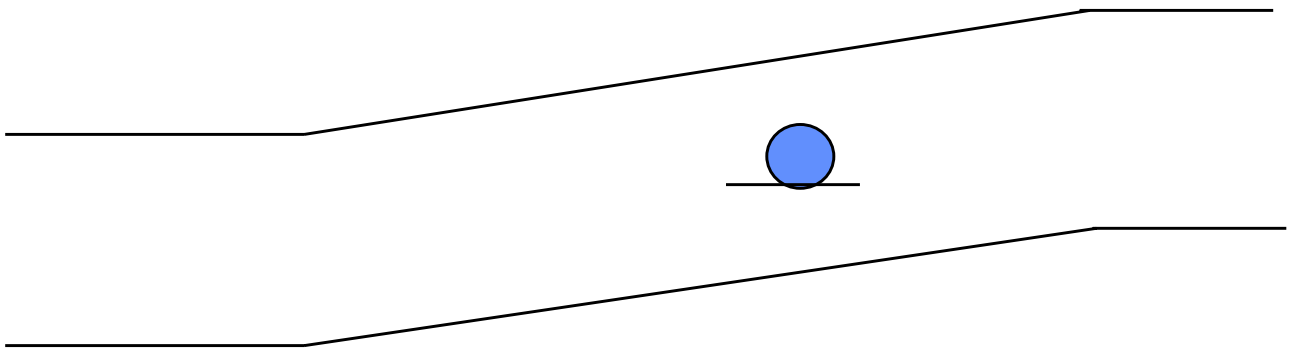

GM-APD reset time

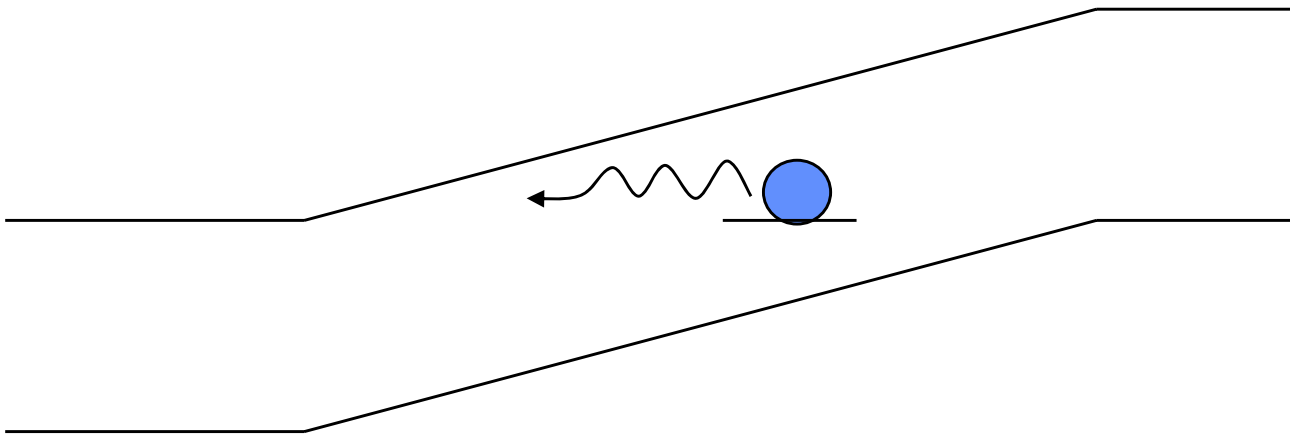

GM-APD reset time

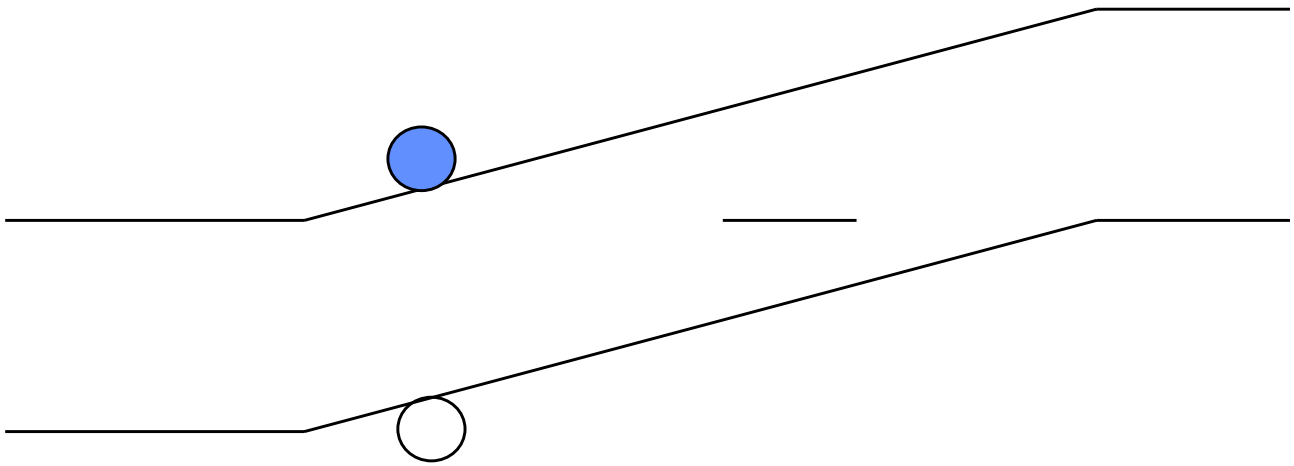

GM-APD reset time

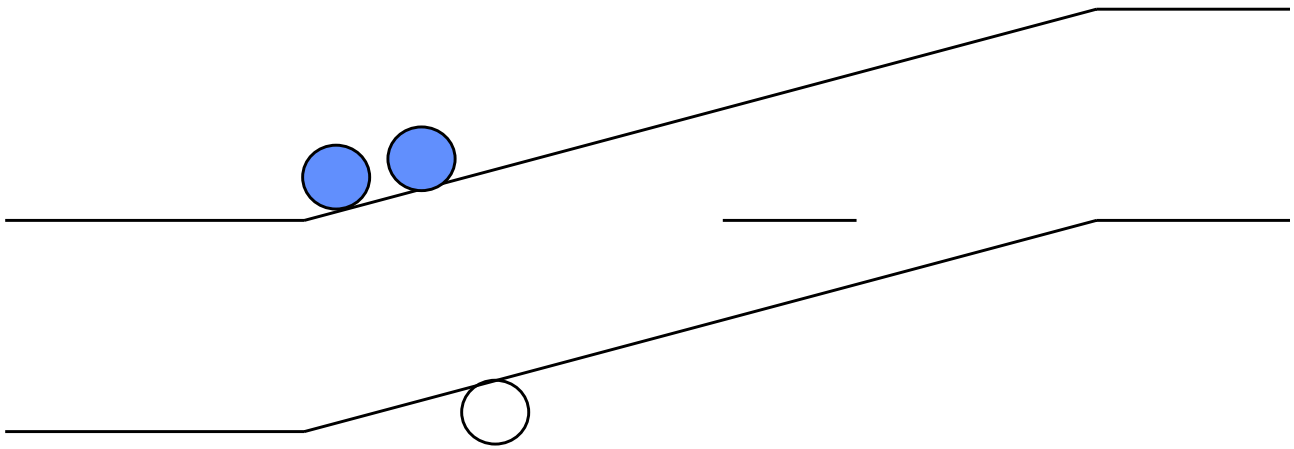

GM-APD reset time

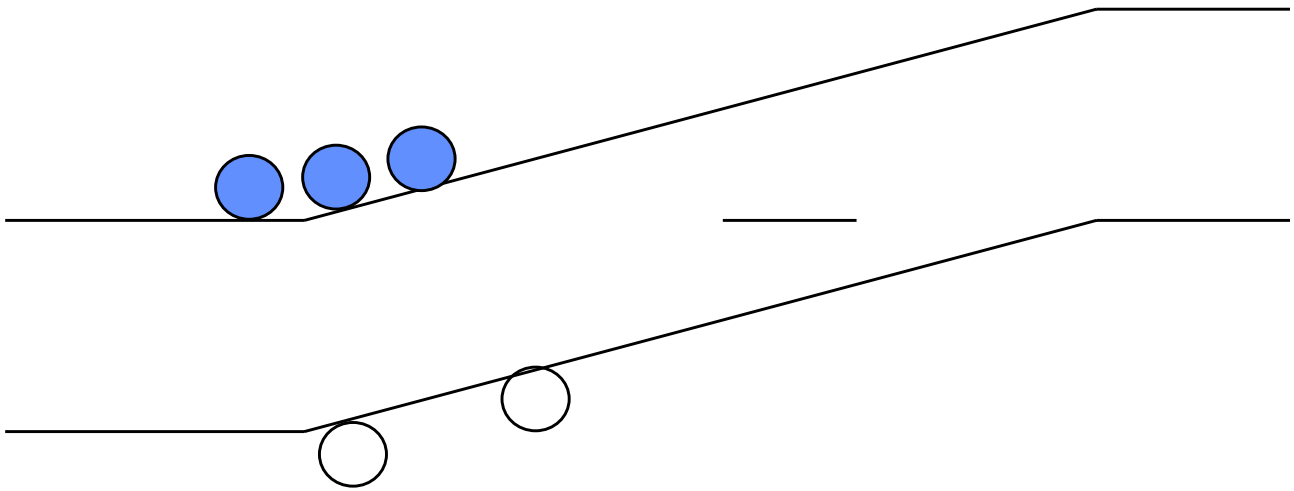

GM-APD reset time

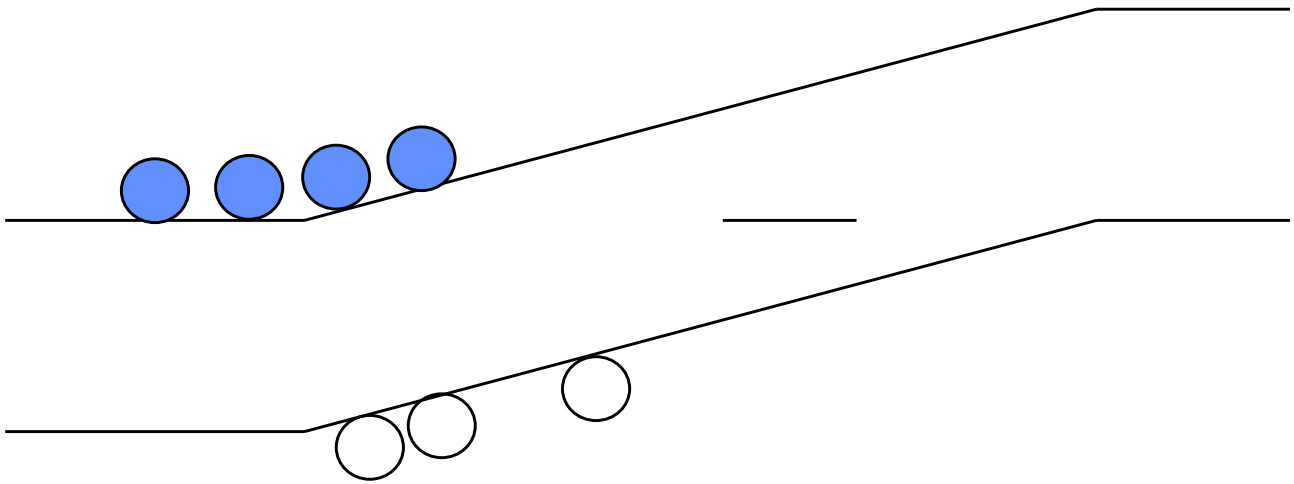

GM-APD reset time

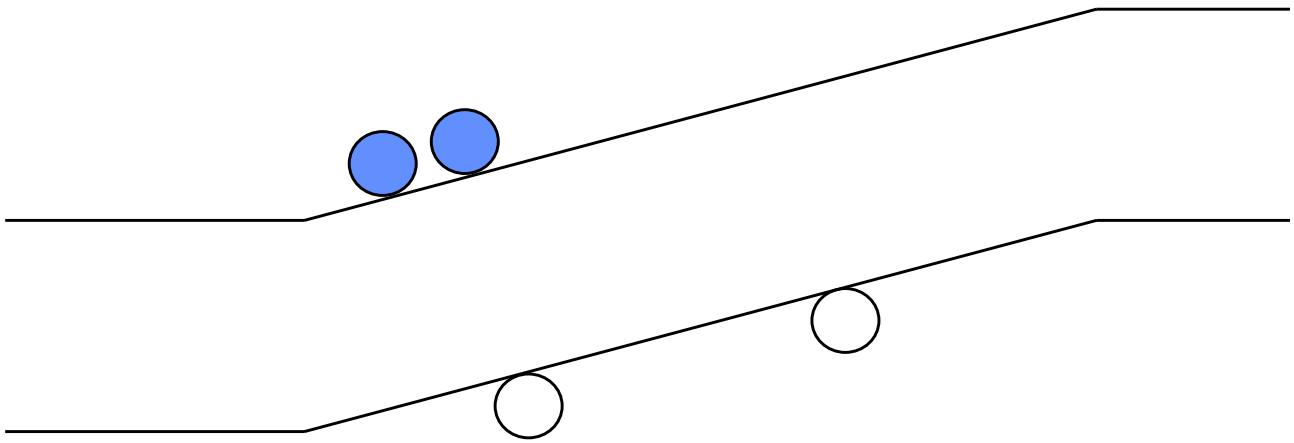

GM-APD reset time

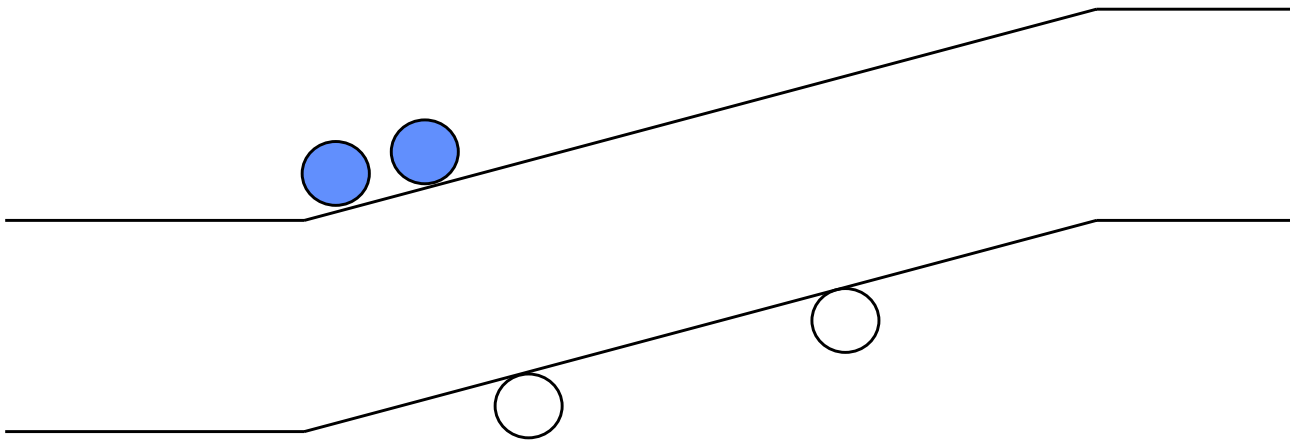

Outline

- Large-format MITLL CCDs for synchrotron applications
- GM-APD arrays for high-flux applications
- Lateral blooming control in large-format CCDs
- Measurements and simulations
- Conclusions

Lateral Blooming Control

450 μm

Lateral Blooming Control (BI)

Blooming barrier ~ +5 V for V_H = +4 V
(sets full well capacity)

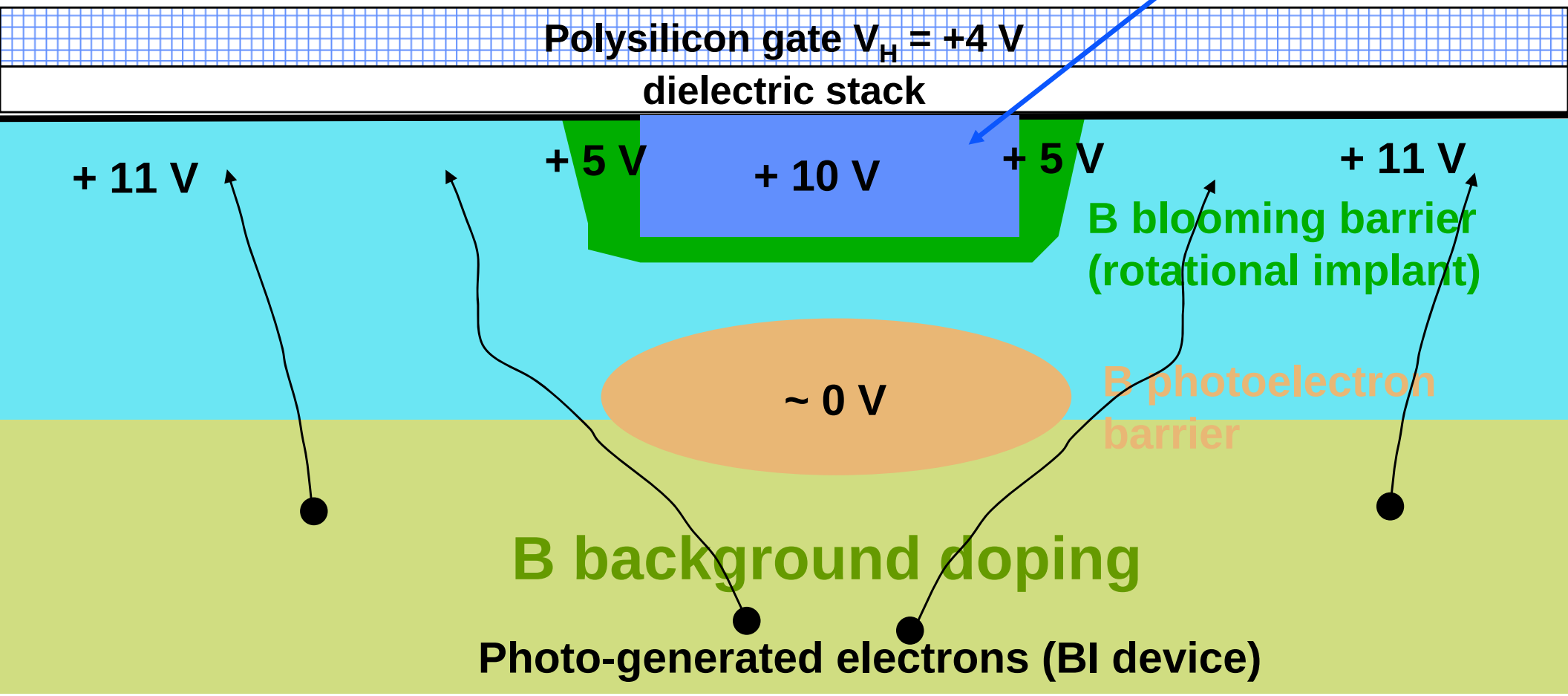

Lateral Blooming Control (FI)

Blooming barrier ~ +5 V for V_H = +4 V
(sets full well capacity)

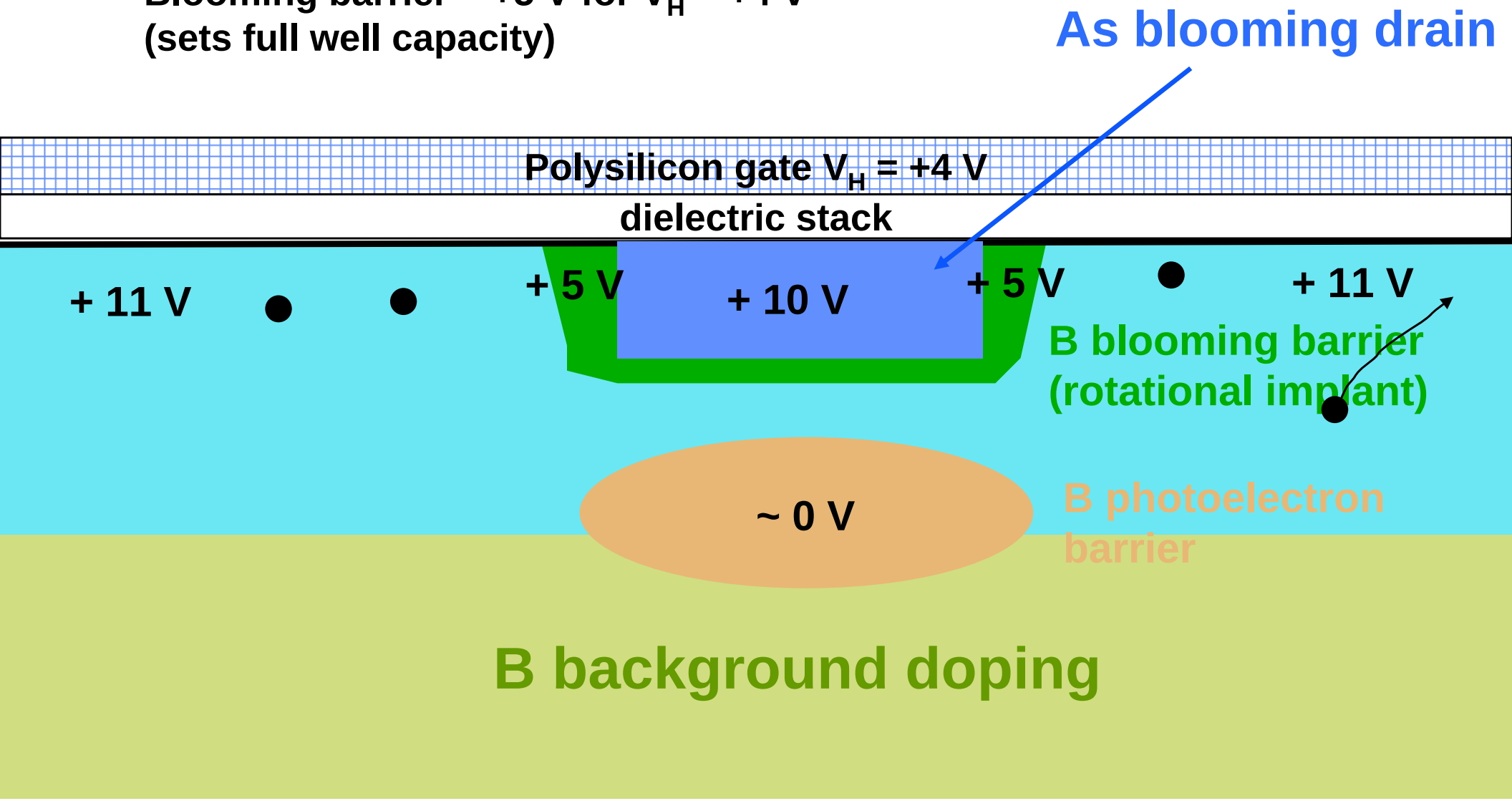

Outline

- MITLL CCDs for space applications
- Lateral blooming control in large-format CCDs
- Measurements
  - Near-single-pixel light source
  - Q vs. T measurements (back-illuminated device)
  - Q vs. T measurements (front-illuminated device)
- Simulations
- Conclusions

Characterizing blooming control

- "Old" (circa 1997) method: flash bright LED into image with blooming control "off"
  - Distortion of spot along columns indicates blooming
- Turn blooming control "on"
  - Absence of spot distortion indicates that blooming control is working
- Assumes current limit to blooming drain

450 μm

Testing limits to blooming control

Blooming control on

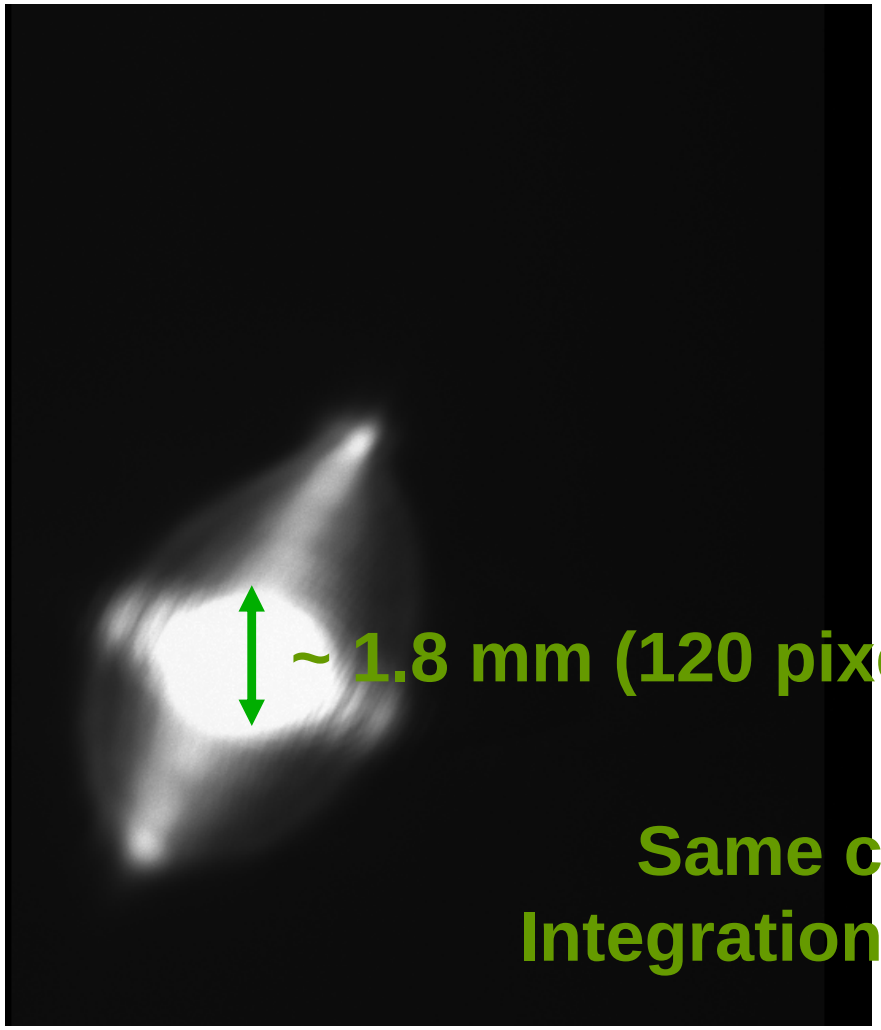

Blooming control off

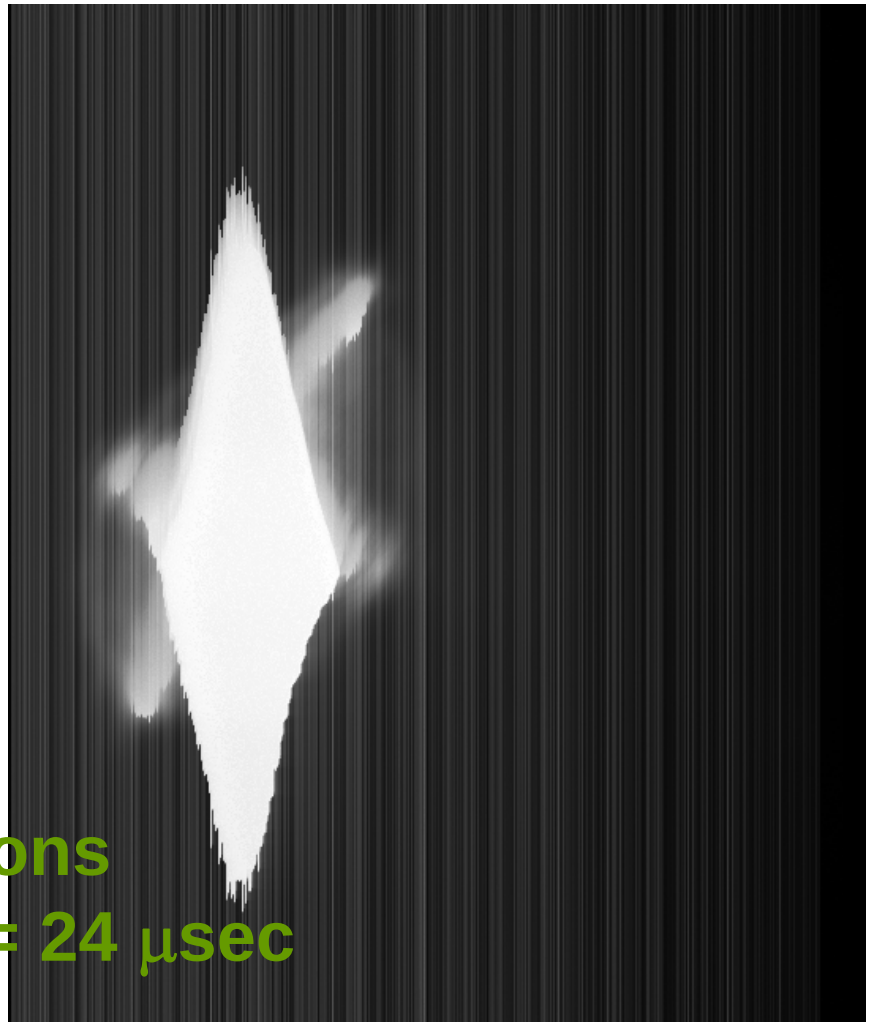

Same conditions
Integration time = 24 μsec

445 nA/column into blooming drain in central column: blooming control functioning well

Disadvantages of testing with large spots

- **Blooming drain can become debiased**
  - **Leads to positional dependence of blooming control (not observed)**
  - **Blooming drain resistance ~ 500 kΩ, so 2 μA flowing into blooming drain produces 1 V drop**
- **Difficult to get single-pixel data**
- **Qualitative**
- **Obviously not relevant to stars**

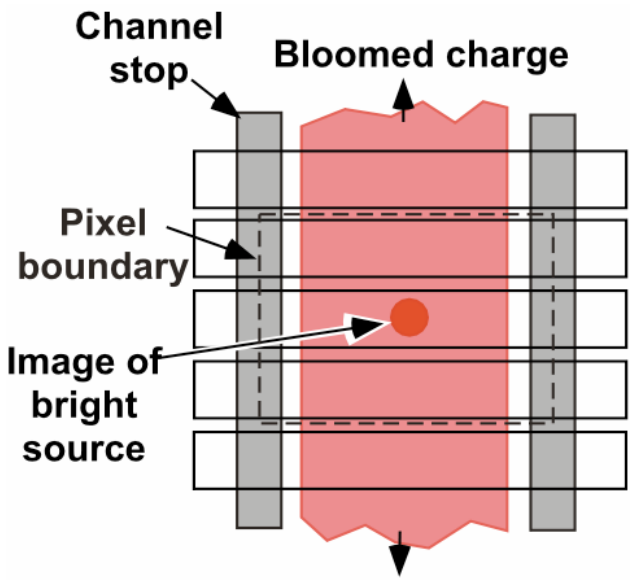

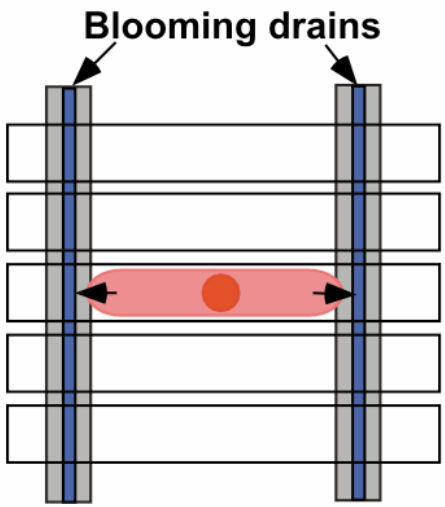

Path to single-pixel measurement

- Tried *edges* (metal masks and cleaved pieces of Si)
  - Image of edge was several pixels wide (scattering, diffraction, etc.).
- 100 μm dia. fiber optic imaged by 7x microscope objective.
  - Spot small (~3-5 pixels FWHM), but not small enough.
  - Smaller fiber an obvious improvement
- Lightshield (metal deposited onto imager, small holes etched) an option
  - Most straightforward method
  - Limited number of samples, not useful for screening

BI lightshield with small apertures

- Diffraction puts ~ 95% (crude estimate) intensity in central pixel
- Charge diffusion in bulk < 1 um for transit times ~ 1 nsec
- Large charge drift/diffusion due to full well might be more significant
- Blooming (occurs only at charge levels around full well)

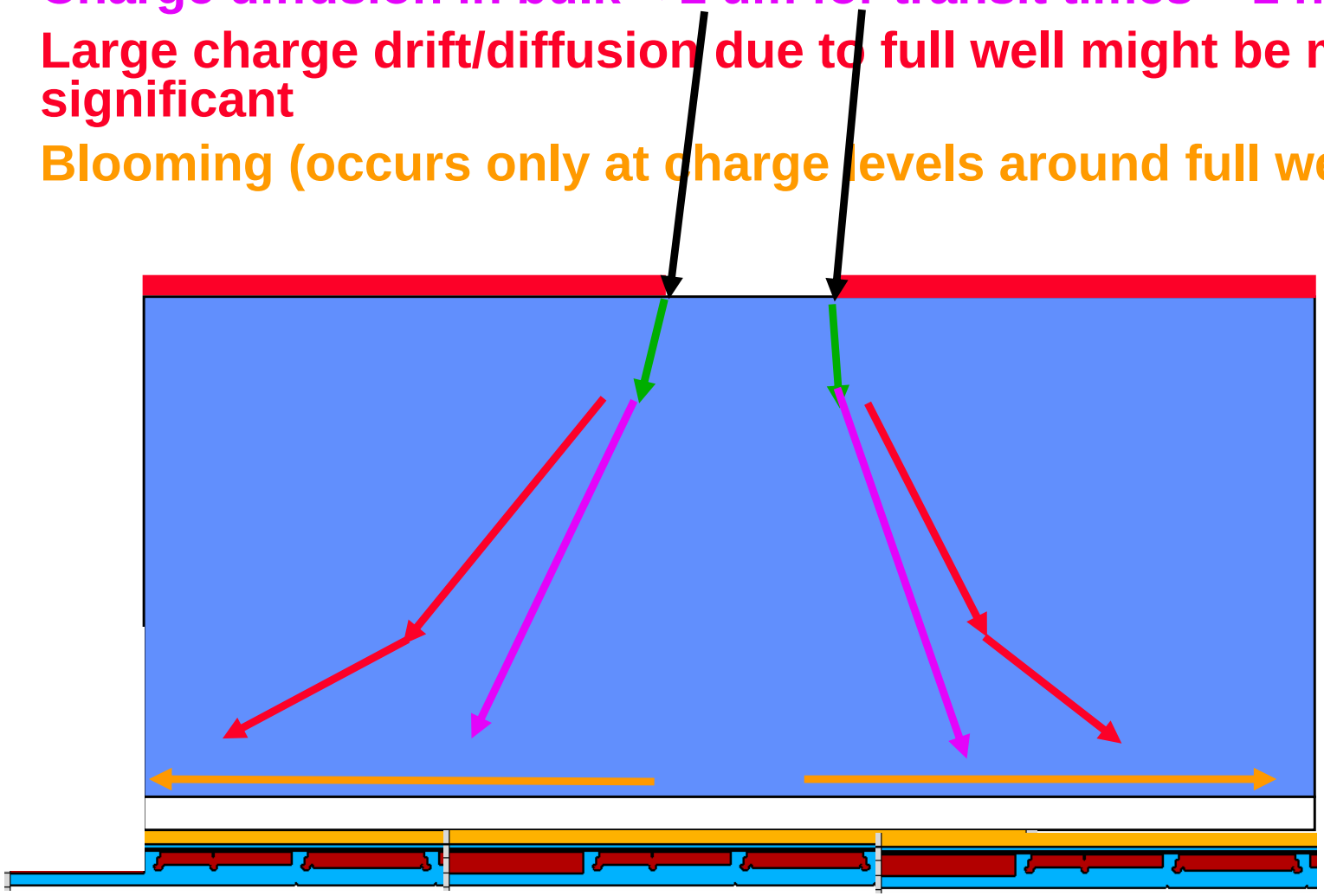

15 um square pixel

Single Pixel Source: New Lightshield

- BI and FI devices
- 3-5 um dia. hole in Al: should be good single pixel source!
- Staggered array to compensate for “alignment by eye”

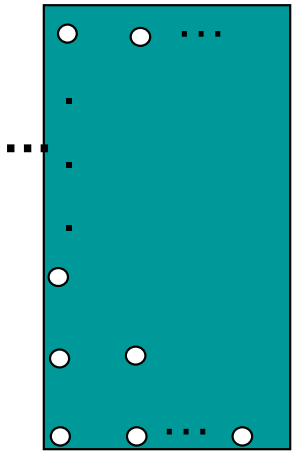

Outline

- Introduction to MITLL CCDs
  - Application to space
- Lateral blooming control in large-format CCDs
- Measurements
  - Near-single-pixel light source
  - Q vs. T measurements (back-illuminated device)
- Simulations
- Conclusions

Q *vs.* T measurements along column

- Close to single pixel illumination (central pixel + leakage into nearest neighbor)!
- Solid lines: all excess charge into neighbor(s); dashed lines: all excess charge into blooming drain
- No charge drift/diffusion

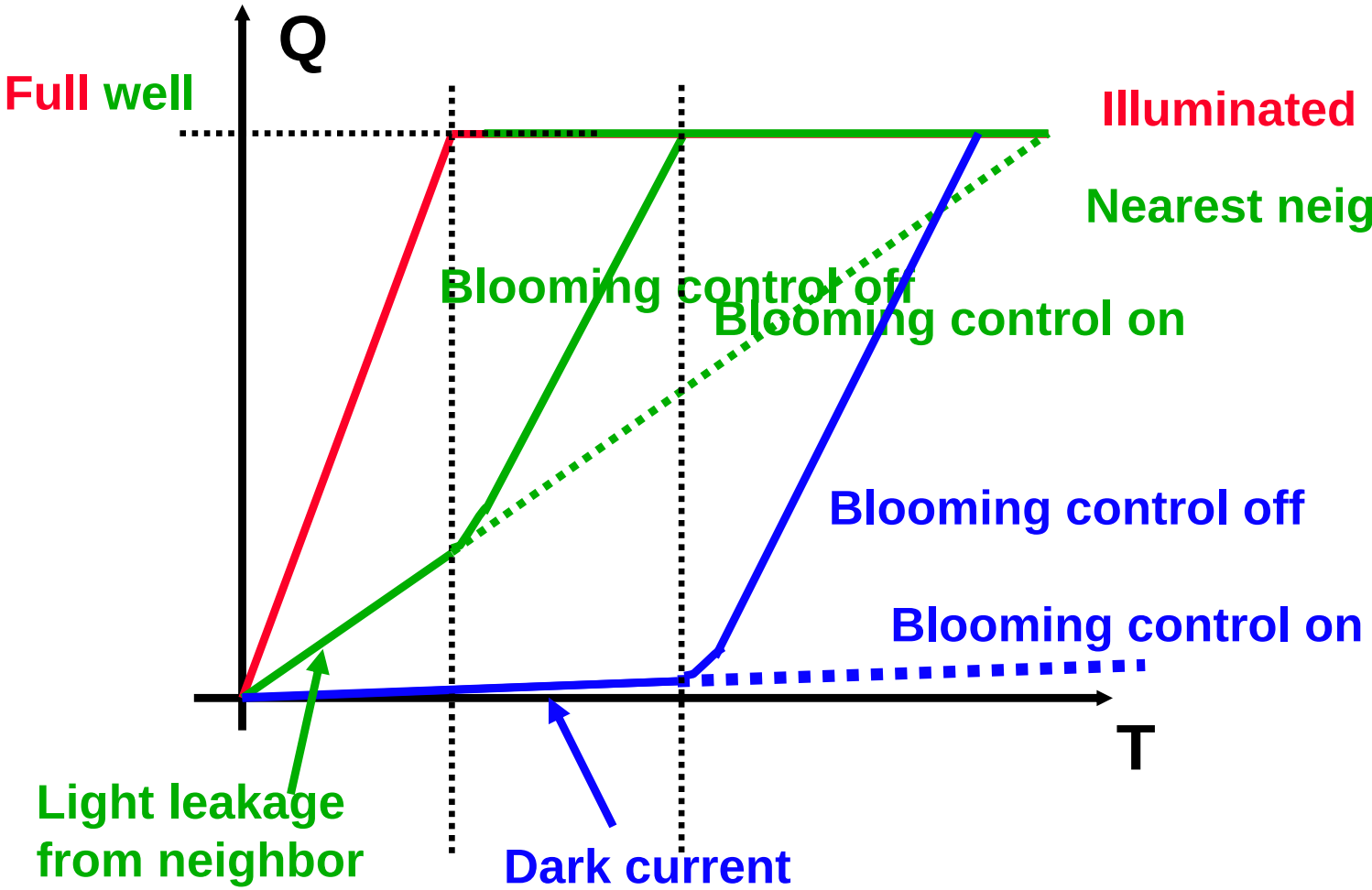

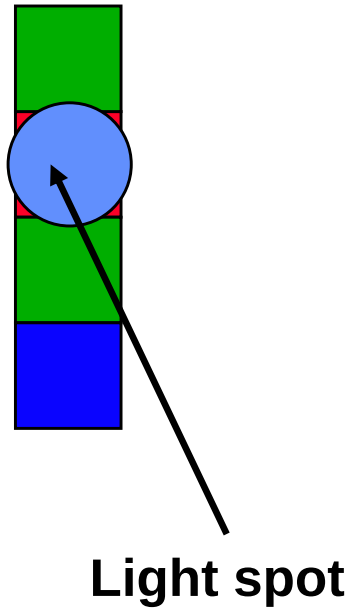

Initial data: 635 nm through BI lightshield

- 635 nm (~ 5 um absorption length)
- Used hole at column 352, various rows on device L2W9C1A
- Determined lower limit to blooming control performance
- FWHM ~ 2 pixels
- 465 nm data similar but shows larger nonlinearities

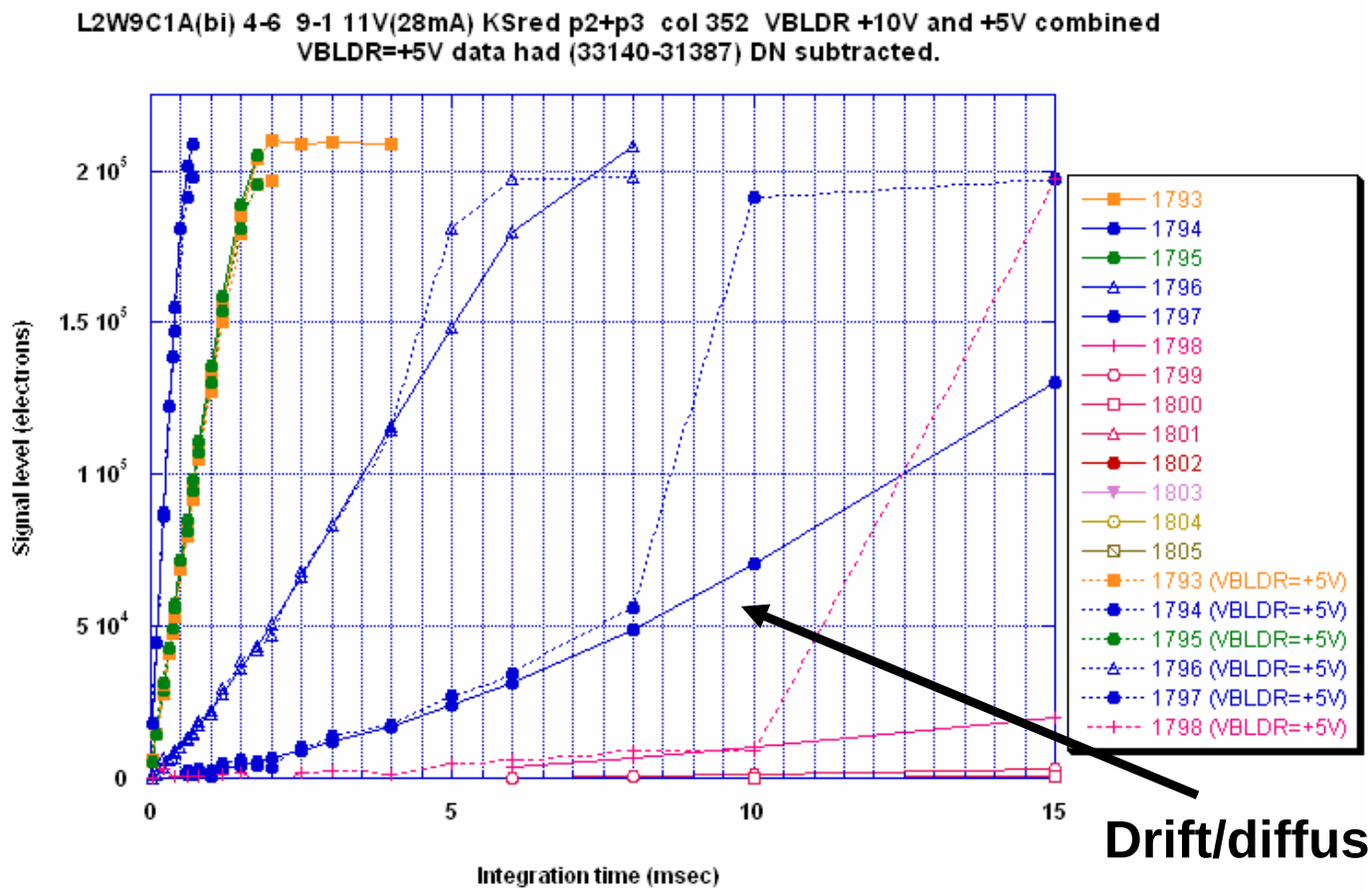

Drift/diffusion in substrate

Outline

- Introduction to MITLL CCDs
  - Application to space
- Lateral blooming control in large-format CCDs
- Measurements
- Simulations
- Conclusions

Drop in electric field from pixel enhances drift/diffusion

- Diffraction
- Charge diffusion
- Large charge drift/diffusion
- Blooming

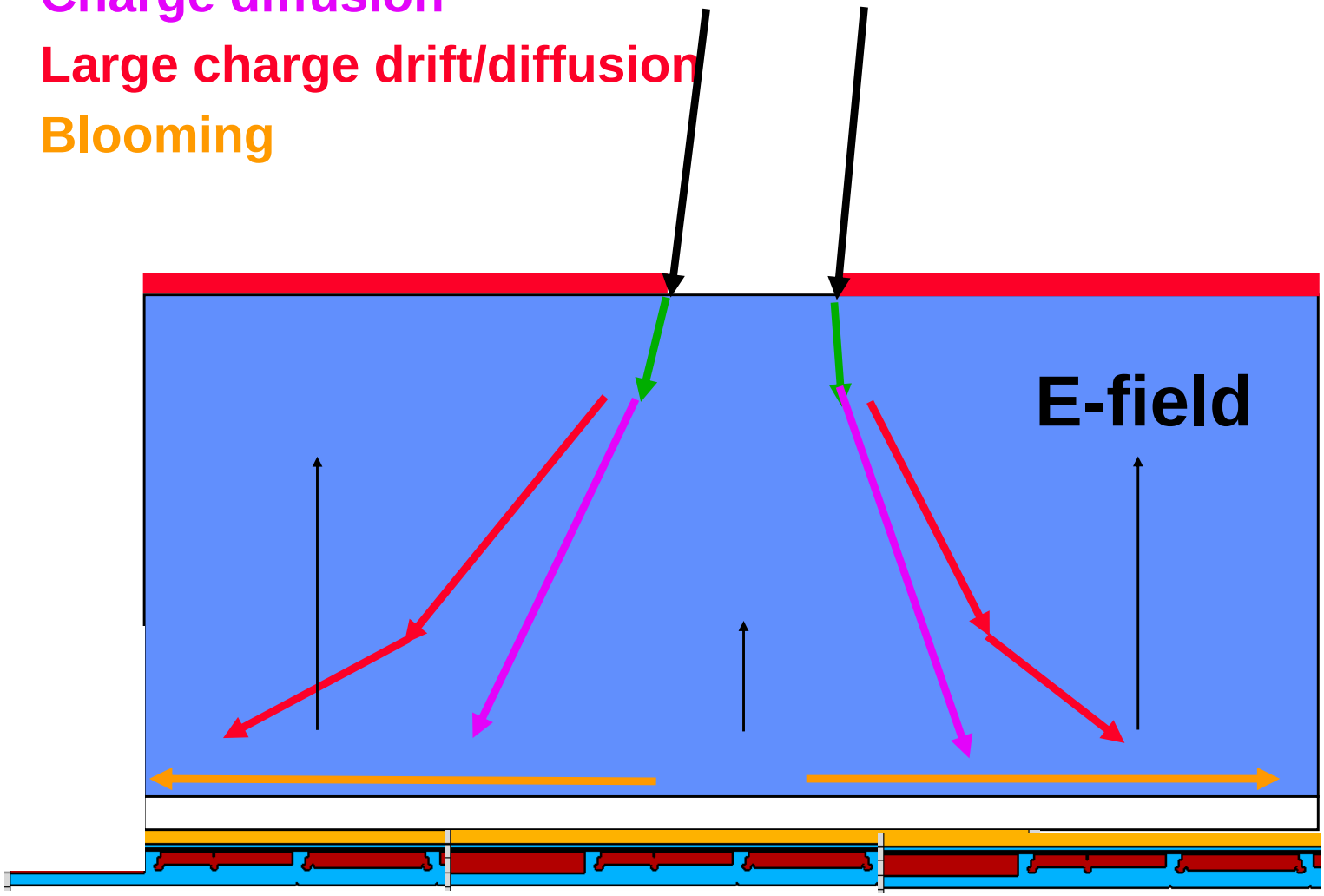

Charge trajectory expected to change from pink to red as electric field in Si drops

15 um square pixel

Simulations of charge motion in CCD

- 2-d simulations of charge motion along columns, and along rows
- Silvaco tools from Silvaco, Inc.
  - ATHENA used for process simulation
  - ATLAS is the Poisson equation solver (solves for fields and charge distribution)

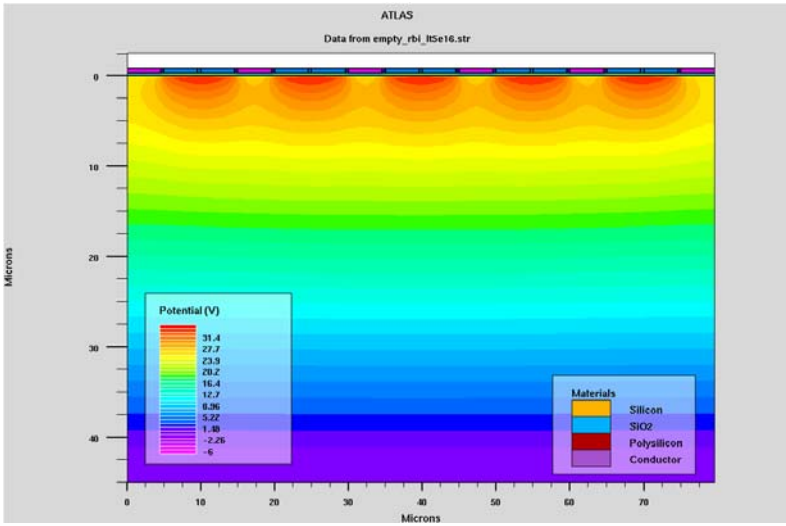

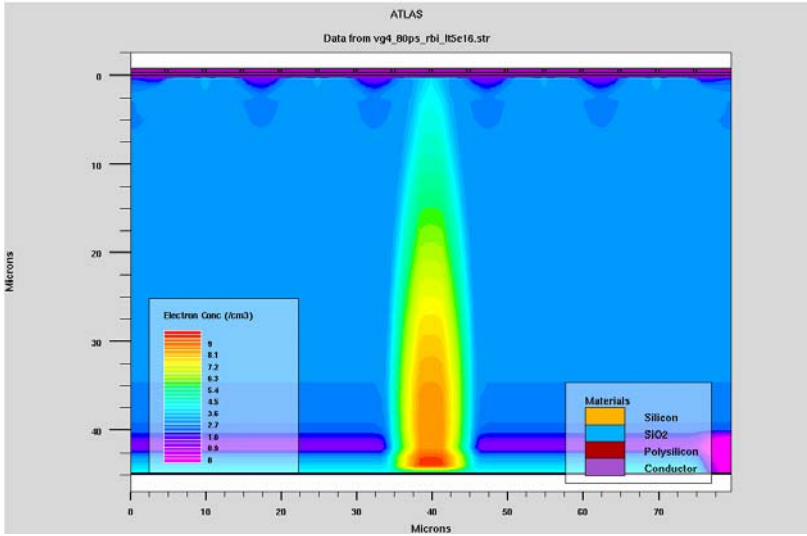

Drop in electric field from pixel enhances drift/diffusion

- Nonlinear Q vs. T predicted due to substrate drift/diffusion
- Confirms experimental results

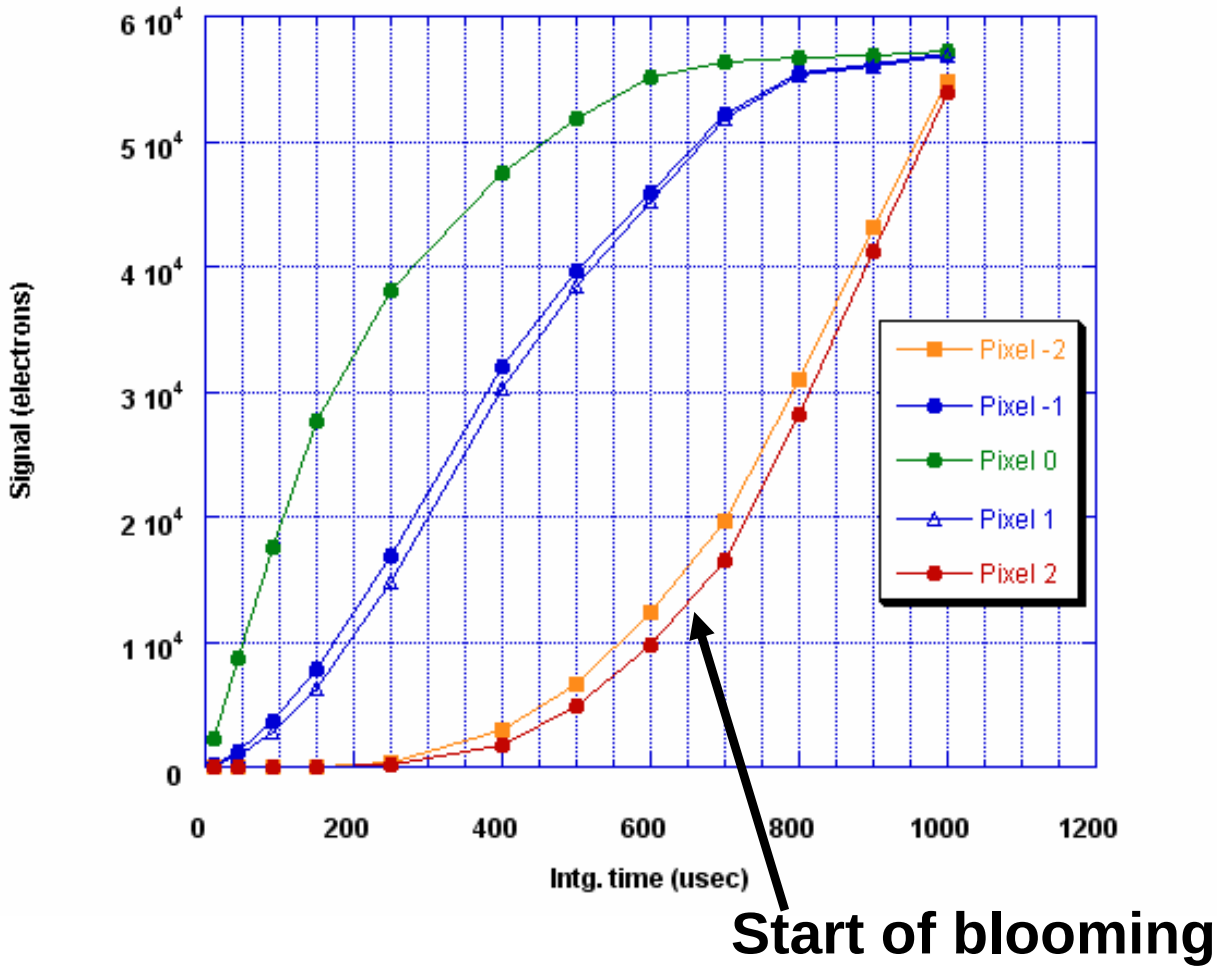

New implant to reduce substrate drift/diffusion suggested

- Blooming barrier ~ +7 V for V_H = +4 V: electric field doesn't drop as low
- Tradeoff: reduction in full well capacity

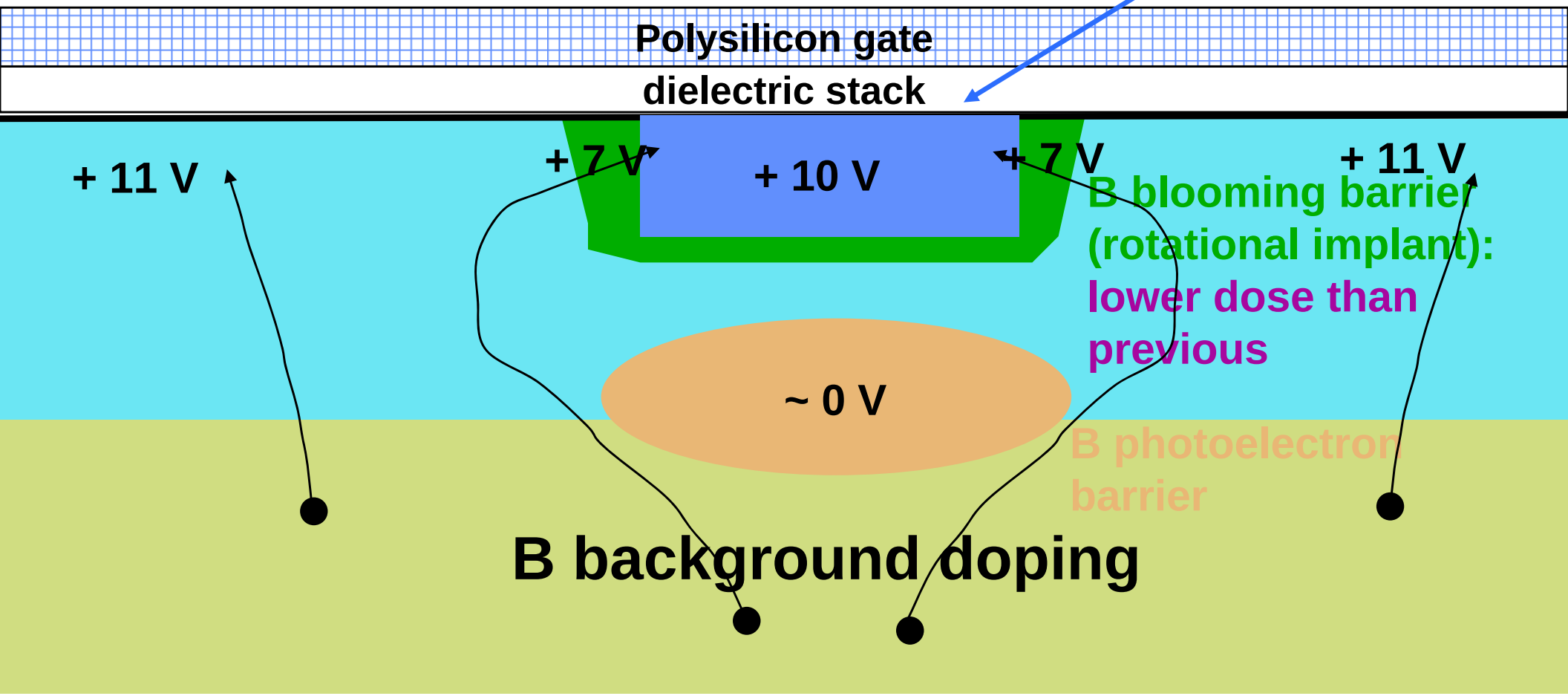

Conclusions

- **Large-format CCDs for x-ray applications designed, fabricated, tested, and delivered by our team**
  - **Simple pixel**
  - **Large format**
  - **Lateral blooming control works well, up to at least 0.5 uA/column**
- **Blooming control tested**
  - **Near-single-pixel illumination source (LED + lightshield)**
  - **Q *vs*. T measurements**
  - **New implants suggested**
- **GM-APD arrays useful for synchrotron holography experiments**
  - **Large dynamic range**
  - **Short reset time**
  - **Technology maturing**